CHALMERS
UNIVERSITY OF TECHNOLOGY

Increasing production of 3-hydroxypropionic acid by modulating the activity of acetyl-CoA carboxylase 1 in *Saccharomyces cerevisiae*

Master's thesis in Biotechnology

JEROEN GIRWAR KOENDJBIHARIE

Department of Biology and Biological Engineering
CHALMERS UNIVERSITY OF TECHNOLOGY
Gothenburg, Sweden 2015

Increasing production of 3-hydroxypropionic acid by modulating the activity of acetyl-CoA carboxylase 1 in *Saccharomyces cerevisiae*

Jeroen Girwar Koendjbiharie

Master's thesis

Department of Biology and Biological Engineering

CHALMERS UNIVERSITY OF TECHNOLOGY

Gothenburg, Sweden 2015

Increasing production of 3-hydroxypropionic acid by modulating the activity of acetyl-CoA carboxylase 1 in Saccharomyces cerevisiae
JEROEN GIRWAR KOENDJBIHARIE

© JEROEN GIRWAR KOENDJBIHARIE, 2015

Department of Biology and Biological Engineering
Chalmers University of Technology
SE-412 96 Göteborg
Sweden
46 (0)31-772 1000

Abstract

3-Hydroxypropionic acid (3-HP) is an attractive chemical that can be produced from biomass, because it can be used as a precursor for a lot of commercially interesting products and thus contribute to a more sustainable, bio-based economy. The synthesis of 3-HP has already previously been shown to be possible in *Saccharomyces cerevisiae* via the heterologous expression of malonyl-CoA reductase (MCR_{Ca}). 3-HP production was further improved via the overexpression of an acetyl-CoA carboxylase 1 double mutant that is no longer phosphorylated by Snf1 (Acc1**). However, malonyl-CoA is also a precursor for fatty acids, and the increased fatty acid production associated with the overexpression of Acc1** is undesirable when aiming to produce 3-HP, and could, at least partly, originate from the presumed association of Acc1 with the cytosolic side of the ER membrane.

It was hypothesized that by bringing the two enzymes, Acc1** and MCR_{Ca}, together with a scaffold, the 3-HP production could be increased by channeling the acetyl-CoA directly towards 3-HP and minimizing the leakage towards fatty acid synthesis. To investigate the use of a scaffold, the following two research questions were proposed:

1) Is it possible to abolish the association of Acc1 with the ER membrane by fusing Acc1 to a docking domain?
2) Is the 3-HP production improved when Acc1 is linked to MCR_{Ca} via a protein scaffold?

Due to the limited time of the project it was not possible to adequately address the proposed questions. However, it was clear that it was not possible to effectively abolish the presumed association of Acc1** with the ER membrane by fusing dockerin a (Da) from *C. thermocellum* endoglucanase to the C-terminus of Acc1**, as it rendered to enzyme non-functional, most likely as the result of incorrect folding. The non-functionality of Acc1**-Da was not an inherent feature of Acc1** when fusing a protein domain to the C-terminus, as Acc1** was still functional with an enhanced green fluorescent protein (eGFP) fused to the C-terminus, as well as to the N-terminus, making the use of a scaffold still a viable strategy to improve the production of 3-HP and other malonyl-CoA derived products.

In parallel, the extent in which Acc1** activity is regulated by the efficiency of its biotinylation by Bpl1 was also investigated. Cultivating *S. cerevisiae* with Acc1** integrated in the genome in the presence of different biotin concentrations did not lead to an increased production of 3-HP, both with and without overexpressing BPL1 via a multiple copy plasmid. This suggested that Acc1** activity is not significantly regulated by its biotinylation. However, to be conclusive about the ACCase activity, it should be directly measured, rather than indirectly, as the 3-HP production is affected by more than just the activity of Acc1**.

Contents

Abbreviations

3-HP	3-hydroxypropionic acid
5-FOA	5-fluoroorotic acid
Acc1	acetyl-CoA carboxylase 1
Acc1**	acetyl-CoA carboxylase 1 (double mutant)
Acc2	acetyl-CoA carboxylase 2
ACCase	acetyl-CoA carboxylase
amp	ampicillin
BC	biotin carboxylase
BCCP	biotin carboxyl carrier protein
BPL1	biotin-apoprotein ligase
Coh a	cohesin a (from *Clostridium thermocellum*)
CT	carboxyl transferase
Da	dockerin a (from *Clostridium thermocellum*)
eGFP	enhanced green fluorescent protein
ER	endoplasmic reticulum
GAPN	non-phosphorylating glyceradehyde-3-phosphate dehydrogenase
HPLC	high-performance liquid chromatography
LB	lysogeny broth (medium)
MCR_{Ca}	malonyl-CoA reductase (from *Chloroflexus aurantiacus*)
PCR	polymerase chain reaction
SD-URA	synthetic defined medium with uracil drop-out
YNB	yeast nitrogen base
YPD	yeast extract peptone dextrose (medium)

1 Introduction

1.1 Relevance of 3-hydroxy propionic acid

In recent years, 3-hydroxypropionic acid (3-HP) has gained significant interest as a bio-based platform chemical (Kumar et al. 2013). It can be used for the production of a variety of commodity chemicals, including malonic acid, acrylamide, and acrylic acid, which is the most promising one from a commercial perspective, as the market value of acrylic acid is estimated to increase from $11,006.6 million in 2013 to $18,824.0 million by 2020 (Clark 2014). Many of those potential products and their derivatives are currently produced from petrochemicals. Bio-based production of 3-HP could therefore decrease the dependence on fossil fuels and contribute towards a sustainable bio-based economy.

In a bio-based economy, biomass, rather than petroleum, forms the basis from which our goods are produced, ranging from high-value added fine chemicals to bulk chemicals (Langeveld et al. 2010). The concept of a bio-refinery plays a key role in a bio-based economy, converting biomass, which typically has a complex composition, into a small subset of building blocks from which a wide range of chemicals and materials can be produced. In 2004, a well-known paper was published by T. Werpy and G. Petersen, where they selected twelve sugar-derived chemicals as candidates for such key building blocks (Werpy & Petersen 2004). 3-HP was one of those twelve candidates, highlighting its potential as a bio-based platform chemical.

1.2 Production of 3-hydroxy propionic acid

Bio-based production of chemicals is typically done with the use of cell factories. Commonly used cell factories for platform chemicals are the model organisms *Escherichia coli* and *Saccharomyces cerevisiae*, which have both, as well as *Klebsiella pneumonia*, been studied for the production of 3-HP (Chen et al. 2014). The use of bacteria, such as *E. coli* has some drawbacks compared to the use of *S. cerevisiae*, of which the lower tolerance to lower extracellular pH is the most relevant for the production of 3-HP, as it is an organic acid. Being able to conduct fermentations at lower pH when producing organic acids is desired, as it lowers the amount of base titrant required as well as the amount of waste (e.g. gypsum) produced for recovering the acid, thus contributing to lower production costs (Maris et al. 2004). Hence, *S. cerevisiae* is the preferred organism.

Several potential synthetic pathways for the production of 3-HP have been proposed (Jiang et al. 2009), and a pathway from malonyl coenzyme A (malonyl-CoA) has previously been proven to be one of the most promising pathways in *S. cerevisiae* (Chen et al. 2014; Jensen et al. 2014). It involved the heterologous expression of malonyl-CoA reductase from the photosynthetic bacterium *Chloroflexus aurantiacus* (MCR_{Ca}), which catalyzes the two reductions, via malonate semialdehyde, required for the conversion of malonyl-CoA to 3-HP. Figure 1 shows the pathway from glucose to 3-HP.

Because both reductions require NADPH and the conversion of glucose to malonyl-CoA yields two NAD(P)H per acetyl-CoA, the pathway from glucose to 3-HP is redox neutral. It does, however, lead to a cofactor imbalance, as MCR_{Ca} can only accept NADPH as a cofactor. Possible ways to overcome this imbalance include mutation of MCR_{Ca} to shift its cofactor specificity, or the introduction of an enzyme/pathway that can transfer electrons between the two different cofactors, such as NAD(P) transhydrogenase (Jiang et al. 2009).

Another issue with the pathway via malonyl-CoA is that there is no net production of metabolic energy, since the production of cytosolic acetyl-CoA costs ATP and the conversion of acetyl-CoA to malonyl-CoA also requires additional ATP. As a consequence, this pathway is not suitable to completely replace ethanol by 3-HP as the main catabolic end-product of anaerobic fermentation. It should theoretically

still be possible to obtain relatively high yields under micro-aerobic/oxygen limited conditions, as the energy required could this way be complemented via the TCA-cycle. Another way to improve the net metabolic energy production would be to engineer the pathway from glucose to (cytosolic) acetyl-CoA to be more ATP efficient, which has been demonstrated to be possible by replacing the native ATP-dependent acetyl-CoA synthetase with the ATP-independent pyruvate dehydrogenase complex from *Enterococcus faecalis* (Kozak et al. 2014). Additionally, the export of 3-HP out of the cell will also require energy (Maris et al. 2004), but that will not be discussed here.

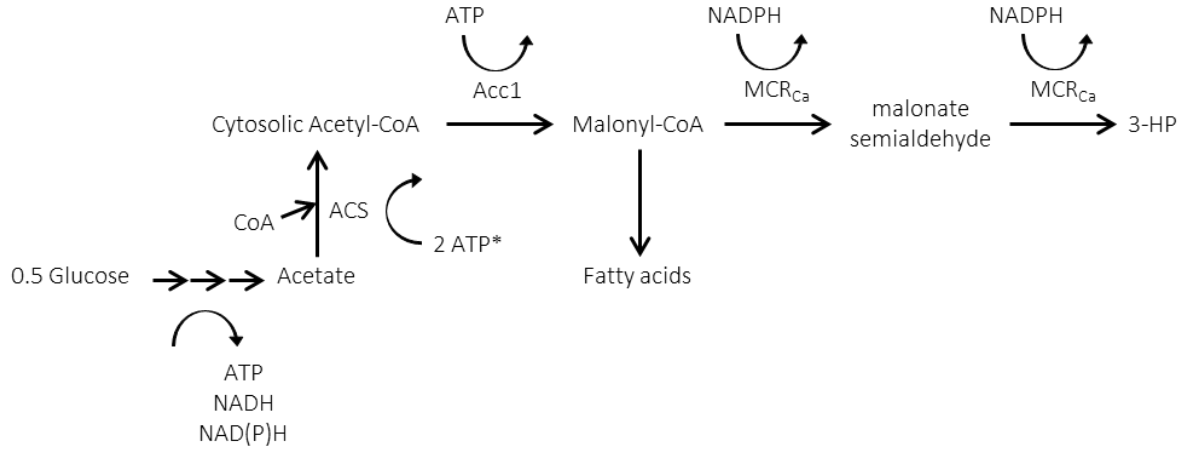

*Figure 1: Pathway from glucose to 3-HP. * acetyl-CoA synthase (ACS) converts 1 ATP into 1 AMP, which is the energy equivalent of 2 ATP to 2 ADP.*

1.3 Malonyl-CoA supply by acetyl-CoA carboxylase

Malonyl-CoA is an intermediate in the central carbon metabolism and is a precursor for several commercially interesting products, such as fatty acids, polyketides and indeed, 3-HP (Krivoruchko & Nielsen 2015; Tehlivets et al. 2007). Malonyl-CoA is produced from acetyl-CoA by acetyl-CoA carboxylase (ACCase; EC 6.4.1.2) in two half reactions. Firstly, the ATP-dependent carboxylation of a prosthetic biotin group and secondly, the transfer of the carboxyl group from biotin to acetyl-CoA (Podkowiński & Tworak 2011).

ACCase plays an essential role in the fatty acid biosynthesis as it catalyzes the rate limiting first step (Hofbauer et al. 2014). Animals and fungi possess two different isoforms of ACCase, i.e. Acc1 and Acc2 (Podkowiński & Tworak 2011). In yeast, the latter is located inside the mitochondria and is encoded by the HFA1 gene (Hoja et al. 2004; Tehlivets et al. 2007). The mammalian Acc2 ortholog has a function that is distinctive from yeast Acc2 as it has an N-terminal peptide that docks onto the outer mitochondrial membrane and is involved in the regulation of beta-oxidation due to the inhibition of carnitine palmitoyltransferase I by malonyl-CoA (Abu-Elheiga et al. 2001; Podkowiński & Tworak 2011). In yeast, however, beta-oxidation takes place in the peroxisome exclusively (Zhang et al. 2010). Acc2 should not be confused with Bpl1, which is sometimes referred to with 'Acc2' and is responsible for the biotinylation of Acc1 (Tehlivets et al. 2007). In *S. cerevisiae*, Acc1 is located in the cytosol and in a study from 1997, Acc1 has been shown to be loosely associated with the cytoplasmic surface of the endoplasmic reticulum (ER), where also the fatty acid elongation takes place (Ivessa et al. 1997; Tehlivets et al. 2007). However, nothing is known about the nature of this interaction. The authors speculate about a protein binding site at the C-terminus of Acc1, because of a heptad repeat between amino acids 2035 and 2067, which is predicted to adopt an α-helical coiled-coil. The design of future experiments to identify the possible protein(s) to which Acc1 might bind is mentioned, but no results from such experiments are available in literature, which leads me to believe that no protein interaction

was identified. More recent, but unpublished experiments from the same researchers using GFP-tagged Acc1 variants suggest that the localization of Acc1 is much more dynamic (Tehlivets et al. 2007). According to the review, "well aerated, glucose-supplemented cells displayed cytosolic localization of the fusion protein, which rapidly aggregated into small foci that collapsed within minutes into one or two large aggregates, when oxygen or glucose became limiting".

ACCase, as mentioned before, catalyzes the rate limiting step in the fatty acid biosynthesis, which makes it a promising target for improving the production of 3-HP and other malonyl-CoA-derived products. In the light of developing cell factories, Acc1 is the more suitable target of the two isoforms, because the engineering of novel pathways should be less complex when located in the cytosol. However, the suitability of Acc2 should not completely be disregarded, since the compartmentalization by organelles could also offer certain benefits, such as favorable specific conditions, less chance of metabolites leaking to different processes and reduction of possible toxic effects of intermediates (Siddiqui et al. 2012).

Having an essential role in the fatty acid biosynthesis, it comes to no surprise that ACCase is strongly regulated (Tong 2005). One enzyme that regulates the activity of ACCase on the protein level is Snf1, the ortholog of AMP-activated protein kinase (AMPK) in mammals. Snf1/AMPK can be described as a cellular energy sensor, as it can sense the ATP/ADP ratio and subsequently modulate anabolic and catabolic pathways to maintain a high ATP/ADP ratio (Hardie 2007).

It has previously been shown that repression of Acc1 by Snf1 can be abolished by the introduction of two mutations in Acc1 at two presumed phosphorylation sites, i.e. Ser659Ala and Ser1157Ala, and that this subsequently led to an increased production of 3HP (Shi et al. 2014). Besides the increased production of malonyl-CoA derived products, overexpression of this Acc1 double mutant (Acc1**) also negatively affected the growth of the cells and an increased accumulation of fatty acids was observed. Based on the report by Hofbauer *et al.* 2014, it is suspected that this affected growth could be due to an increased ratio of the C18:C16 fatty acid acyl chain length distribution, besides the more obvious effects of an increased 3-HP accumulation.

1.4 Structure of acetyl-CoA carboxylase 1

Eukaryotic Acc1 is a large protein that is made up from four distinctive domains, similar to prokaryotic ACCase, which is made up from four separate subunits. The four different domains form three different modules: Biotin carboxyl carrier protein (BCCP), biotin carboxylase (BC), and carboxyl transferase (CT), which is made from two domains (alpha and beta) (Podkowiński & Tworak 2011). A schematic model of ACCase with the different domains is shown in figure 2, together with the linear architecture of Acc1 from *S. cerevisiae*.

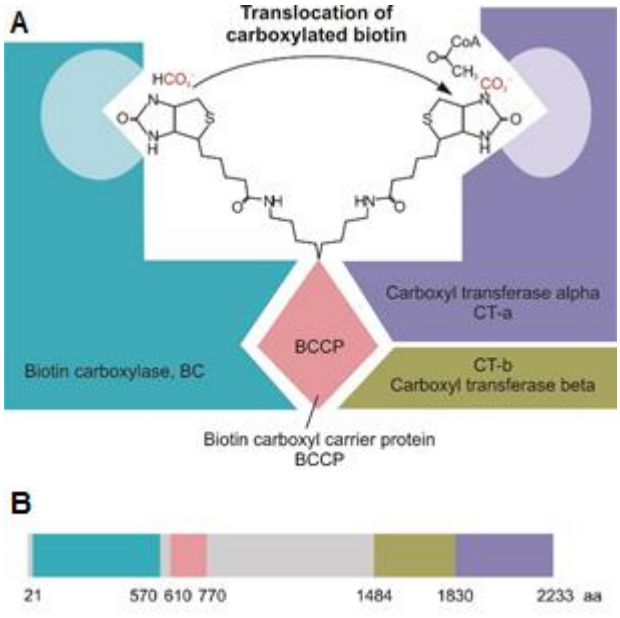

Figure 2: (A) Schematic model of acetyl-CoA carboxylase with the four different domains. (B) Linear architecture of the acetyl-CoA carboxylase protein from S. cerevisiae. (Podkowiński & Tworak 2011)

1.5 Biotinylation of acetyl-CoA carboxylase 1

As mentioned earlier, Acc1 is a biotinylated enzyme. Biotin is covalently attached to the BCCP domain by biotin-apoprotein ligase (Bpl1), which is encoded by the BPL1 gene and is sometimes referred to with 'Acc2'. Biotinylation is required for ACCase activity, and as it appears (without data shown) that not all Acc1 in the cell is biotinylated, the process of biotinylation could be an additional regulatory mechanism for the activity of Acc1 (Tehlivets et al. 2007). Therefore, the biotinylation of Acc1 is another potential target to improve its activity and in turn increase the 3-HP production, as was demonstrated with the Acc1 double mutant that is no longer repressed by Snf1. However, simultaneous overexpression of Acc1 and Bpl1 is said to render the cells inviable (Tehlivets et al. 2007).

1.6 Aim of the study

The aim of this study is the engineering of the central carbon metabolism in *S. cerevisiae* by further modulating the activity of the key enzyme Acc1, in order to improve the production of 3-HP and possibly decrease the negative effects on the natural fatty acid biosynthesis.

More specifically, the aim was to see if the flux of malonyl-CoA towards 3-HP could be increased by bringing the two enzymes, Acc1** and MCR_{Ca}, together using synthetic protein scaffolds that bind to docking domains that are fused to the two enzymes. This should, hypothetically, not only increase the flux of malonyl-CoA via MCR_{Ca} towards 3-HP, due to the spatial proximity, but it should also decrease the flux towards fatty acid biosynthesis by abolishing the association of Acc1 with the ER, where the fatty acid elongation takes place (Tehlivets et al. 2007).

In parallel, the effect of biotinylation of Acc1** by Bpl1 on the activity of Acc1** was investigated to see whether a limited biotinlyation could be limiting the activity of Acc1**.

To summarize, the following research questions were proposed:

1) Is it possible to abolish the association of Acc1 with the ER membrane by fusing Acc1 to a docking domain?
2) Is the 3-HP production improved when Acc1 is linked to MCR_{Ca} via a protein scaffold?
3) To what extend is Acc1** activity regulated by the efficiency of its biotinylation by Bpl1?

To answer the proposed questions, the Acc1** gene was integrated in the genome of *S. cerevisiae* using different conformations. It was fused to GFP to try to investigate to localization of the enzyme in the cell and at the same time the gene was also fused to the 'dockerin a' protein (Da), which can bind to the 'cohesion a' protein (coh a). These proteins are derived from *Clostridium thermocellum* and are part of a cellulosome, where Da is the native dockerin of endoglucanase CelA (Tsai et al. 2010). The plan was to fuse MCR_{Ca} to another dockerin, and to fuse the different corresponding cohesins to each other to create a synthetic scaffold.

To investigate the effect of biotinylation on the production of 3-HP, cells expressing Acc1** were grown in different concentrations of biotin in combination with overexpression of Bpl1, the protein responsible for biotinylation.

2 Materials and methods

2.1 Strains

All *S. cerevisiae* strains constructed in this study were derived from CEN.PK113-5D strain, which is auxotrophic for uracil. Preparation of frozen stock was done by making 1 mL aliquots containing 812 µL of exponentially growing cells and 188 µL 80% (v/v) glycerol that were stored at -80 °C. Table 2 lists all the strains used in this study, and figure 3 shows the architecture of the integrated gene constructs. For clarity, the strains are usually referred to by the name of integrated construct rather than the cryptic strain name.

Table 1: List of all the strains and plasmids used in this study. Figure 3 shows the architecture of the integrated gene constructs. The plasmid map of pJK1 can be found in figure A3.

Strain name	Genotype	Integrated construct	Plasmid	Origin
CEN.PK 113-5D	MATa *ura3-52 HIS3 LEU2 TRP1 MAL2-8c SUC2*			
JK0111	CEN.PK 113-5D	Acc1**	pYC1	This study
JK0112	CEN.PK 113-5D	Acc1**	pJK1	This study
JK0211	CEN.PK 113-5D	Acc1**-Da	pYC1	This study
JK0300	CEN.PK 113-5D	eGFP-Acc1**		This study
JK0311	CEN.PK 113-5D	eGFP-Acc1**	pYC1	This study
JK0400	CEN.PK 113-5D	eGFP-Acc1**-Da		This study
JK0001	CEN.PK 113-5D		pYC1	This study
JK0002	CEN.PK 113-5D		pJK1	This study
JK0500	CEN.PK 113-5D	Acc1**-eGFP		This study
JK0511	CEN.PK 113-5D	Acc1**-eGFP	pYC1	This study
JK0600	CEN.PK 113-5D	Da-Acc1**-eGFP		This study
JK0711	CEN.PK 113-5D	Da-Acc1**	pYC1	This study
JK0811	CEN.PK 113-5D	Acc1**-Da-14	pYC1	This study
JK0900	CEN.PK 113-5D	eGFP-Da		This study
JK1000	CEN.PK 113-5D	eGFP-Da-14		This study
Plasmid name	**Genes overexpressed**		**Origin**	
pYC1	MCR_{Ca}		(Chen et al. 2014)	
pJK1	MCR_{Ca}, BPL1		This study	

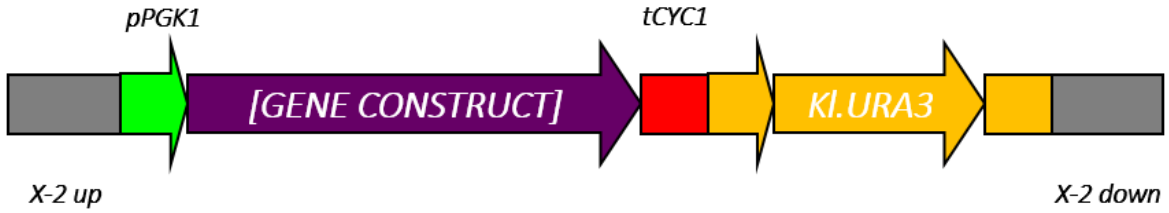

Figure 3: The architecture of the integrated gene constructs. X-2 refers to integration site 2 in chromosome X, as described by Mikkelsen et al. (2012).

2.2 Strain construction

Transformation of yeast was done using the standard LiAc/SS carrier DNA/PEG method (Gietz & Schiestl 2007). For genomic integration of constructs, the homologous region X-2, selected by Mikkelsen et al. 2012 for stable integration, was used. The upstream and downstream homologous regions were amplified from the X-2 integration plasmid, including the URA3 selection marker, which was flanked by

direct repeats. All constructs used the PGK1 promoter and the CYC1 terminator. If the strain was to be subsequently transformed with a plasmid harboring the URA3 selection marker, the integrated marker was first looped out using plates containing 5-FOA (Fonzi & Irwin 1993).

For genomic integration of the constructs, several smaller fragments with at least 30 bp overlap were used for the transformation that would be assembled via homologous recombination in yeast. Amounts of the individual fragments were chosen such that the ratio compared to the fragment harboring the selective marker was at least 2:1, in order to minimize the occurrence of false positives. The primers used for the construction of the different constructs are listed in table A3.

Strains were selected using synthetic dextrose plates lacking uracil (SD-URA), and colonies were verified using colony PCR. When constructs were confirmed with PCR, but the strain didn't show the expected phenotype, (parts of) the constructs were also verified by sequencing.

2.3 Media

Synthetic 'Delft' medium: 20 g/l glucose, 7.5 g/l $(NH_4)_2SO_4$, 14.4 g/l KH_2PO_4, 0.5 g/l $MgSO_4$ * $7H_2O$, 2 ml/l trace elements solution and 1ml/l vitamins solution, with the pH adjusted to 6.5 (Verduyn et al. 1992).

YPD: 10 g/l yeast extract, 20 g/l peptone, 20 g/l glucose.

SD-URA: 6.9 g/l YNB (w/o amino acids), 20 g/l glucose 0.77 g/l CSM-Ura, (20 g/l agar), with the pH adjusted to 5.5 – 6.0.

5-FOA: 6.9 g/l YNB (w/o amino acids), 20 g/l glucose 0.77 g/l CSM-Ura, 50 mg/l uracil, 0.75 g/l 5-FOA, (20 g/l agar), without adjusting the pH.

LB + amp: 10 g/l peptone/tryptone, 10 g/l NaCl, 5 g/l yeast extract, 80 mg/l, (16 g/l agar), with the pH adjusted to 7.0.

2.4 Shake flask cultivation

Shake flask cultivation of *S. cerevisiae* was carried out in 100 mL Erlenmeyer flasks containing 20 mL of synthetic medium. Shake flasks were incubated at 30 °C on a KS 501 orbital shaker (IKA-Werke, Staufen, Germany) at 200 rpm. Pre-cultures were grown in YPD. Cells were inoculated with a starting OD_{600} of 0.02. Inocula were prepared by centrifuging pre-cultures at 3000 rpm for 5 minutes and resuspending them in synthetic medium. To determine the volume of inoculum to be added to the shake flasks, the following equation was used: [volume inoculum] = [volume medium] * [starting OD] / ([OD inoculum] – [starting OD]). For the growth rate measurements 30 mL of medium was used instead of 20 mL, and a starting OD_{600} of 0.01.

2.5 Molecular biology procedures

For the construction of the pJK1 plasmid, the *BPL1* gene was cloned from *S. cerevisiae* using Phusion polymerase with primers that harbored restriction sites (See table A4 for the primers used). Both the cloned *BPL1* gene and the vector (pYC1, (Chen et al. 2014)) were digested with the *NotI* and *PacI* restriction enzymes and then ligated, forming the pJK1 plasmid with *BPL1* controlled by the *PGK1* promoter (see figure A3 for the plasmid map). The ligation mixture was subsequently used to transform competent DH5α *E. coli* cells using heat shock. For plasmid extraction from *E. coli* the plasmid extraction kit from Thermo Scientific was used according to the protocol.

Cloning and amplification of DNA fragments was done using Phusion high-fidelity polymerase (Thermo Scientific, Waltham, MA, USA) in a S1000 thermocycler (BioRad) and for the fusion of different DNA fragments, PrimeSTAR polymerase (TaKaRa) was used. The subsequent purification of PCR products was

done either using the PCR purification kit from Thermo Scientific or using agarose gel electrophoresis and the Gel extraction kit from Thermo Scientific.

2.6 Analytical methods

DNA concentrations were determined using NanoDrop2000 (Thermo Scientific) spectrophotometer, by measuring the absorbance at 260 nm.

The cell density and growth were determined by measuring the optical density at 600 nm (OD_{600}) in a cuvette using a GENESYS 20 spectrophotometer (Thermo Scientific). When necessary, samples were diluted to stay within linear range of OD_{600} 0.400.

The concentrations of 3-HP, glucose and other external metabolites were measured using a Dionex UltiMate 3000 HPLC system (Dionex Softron GmbH, Germering, Germany) with an Aminex HPX-87H column (BioRad, California). 0.5 mM H_2SO_4 was used as the mobile phase, at a flow rate of 0.5 mL/min. The temperature of the column was set at 65 °C. UV and the refractive index (RI) were used for detection. The injection volume was 1 µL. The small injection volume is required to adequately separate 3-HP and glycerol. As a result, however, the detected peaks are very small and could negatively impact the accuracy and precision of the obtained result.

2.7 Microscopy

For the microscopy, cells were cultivated in liquid medium. To get a higher cell density for examination under the microscope, samples were centrifuged and subsequently resuspended after most of the medium was poured off. A Leica DMI4000B inverted microscope (Leica Microsystems GmbH, Wetzlar, Germany) was used. Imaged were recorded with a Leica DFC360 FX camera in combination with the Leica application suite software.

2.8 Flow cytometry

For flow cytometry, cells were diluted in water to an OD_{600} of 0.02 and 200 µl was used for analysis with a flow cytometer. The OD_{600} of the cultures was around 4 when the samples were taken.

3 Results

3.1 Acc1 localization

According to a report from 1997, Acc1 is localized in the cytosol, but loosely associated with the cytosolic side of the ER membrane (Ivessa et al. 1997). The machinery for the fatty acid elongation is also located on the cytosolic side of the ER (Tehlivets et al. 2007; Hofbauer et al. 2014), as a result, overexpression of Acc1** might cause the produced malonyl-CoA to be steered towards the fatty acid production, rather than the production of 3-HP. It was hypothesized that this association of Acc1 with the ER membrane could be abolished by fusing a protein to the C-terminus of Acc1.

To test this hypothesis, several strains were constructed with Acc1** integrated into the genome, with and without dockerin a (Da; from *Clostridium thermocellum* (Tsai et al. 2010)) fused to the C-terminus. Da was used, because in future experiments a synthetic scaffold was to be used to which Da would attach. In addition, eGFP was fused to the N-terminus of Acc1**, in order to observe a possible change in localization using fluorescence microscopy.

In order to construct the strains with the four different Acc1** variants (Acc1**, Acc1**-Da, eGFP-Acc1**, eGFP-Acc1**-Da), four linear DNA fragments were constructed using fusion PCR. Two upstream parts, with and without eGFP, and two downstream parts, with and without Da. The upstream and downstream parts had an overlapping region of 157 base pairs in the middle of the Acc1** gene. The four strains were constructed by combining the two upstream fragments with the two downstream fragments, as shown in figure 4. All construct used pPGK1 and tCYC1 as promoter and terminator, respectively. The downstream fragment contained a URA3 auxotrophic marker that was looped out on 5-FOA plates after successful transformation.

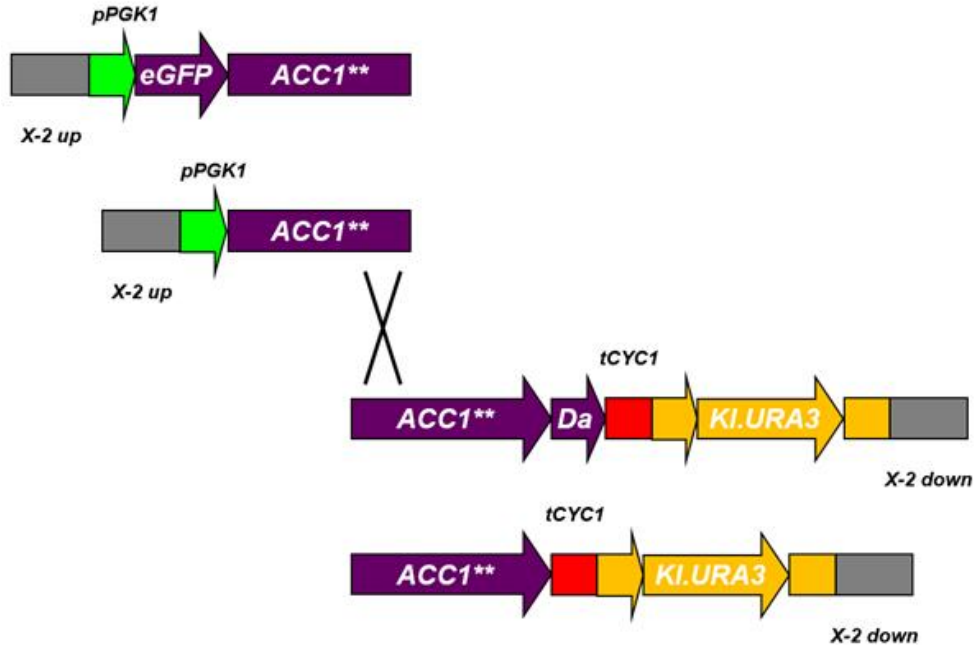

*Figure 4: Schematic presentation of the linear DNA fragments used to construct the strains with the four different Acc1** variants (Acc1**, Acc1**-Da, eGFP-Acc1**, eGFP-Acc1**-Da).*

The two strains with eGFP fused to the N-terminus of Acc1** were investigated using fluorescence microscopy. The results are shown in figure 5. Several pictures with increasing exposure times were taken, because the intensity of fluorescence was significantly different between the two different strains.

	eGFP-Acc1** JK0300	eGFP-Acc1**-Da JK0400
100 ms	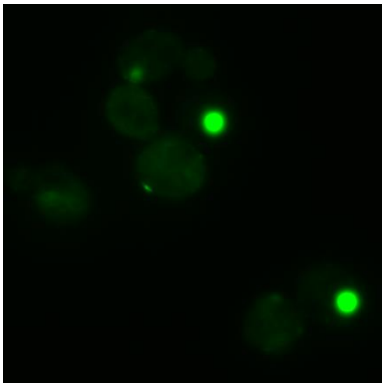	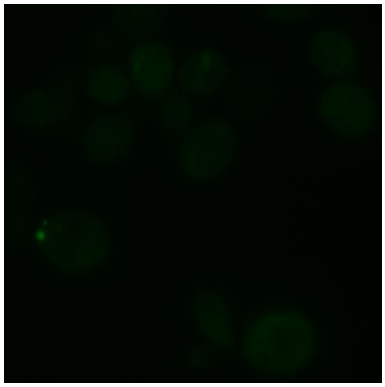
150 ms	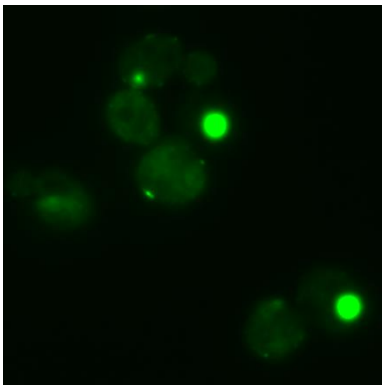	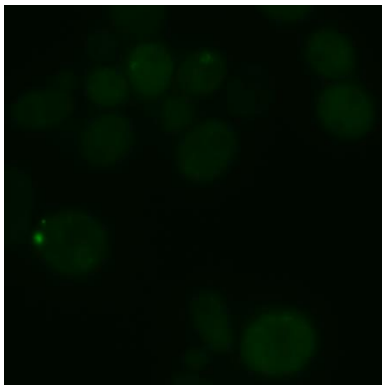
200 ms	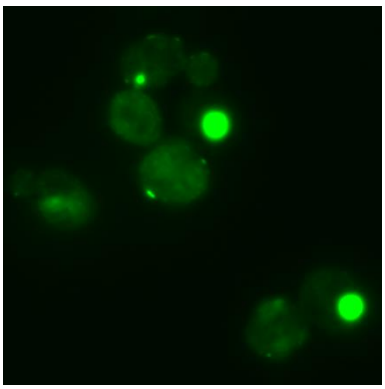	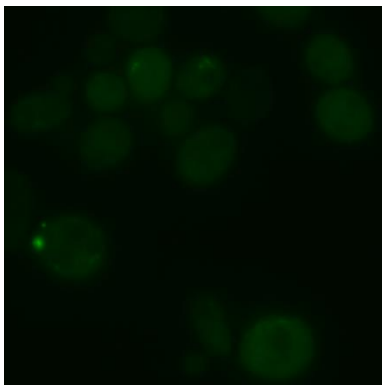
DIC		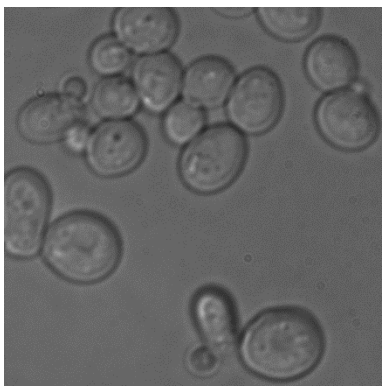

*Figure 5: Results of the fluorescence microscopy of Acc1** with eGFP fused to the N-terminus and with and without Da fused to the C-terminus (JK0400 and JK0300). Fluorescent photos were taken with different exposure times, namely 100, 150 and 200 ms. Photos in the bottom were taken using differential interference contrast (DIC) microscopy.*

Figure 5 clearly shows a difference between the two strains. Most notably is the difference in intensity: the cells with Da fused to Acc1** have a significantly lower fluorescence intensity. Additionally, the distribution of the fluorescence also seems to be more homogenous. In the strain without Da fused to the C-terminus of Acc1** some very bright spots can be observed in a large fraction of the cells. Those bright spots are thought to be aggregates.

These results can have several implications. The more homogenous distribution could support the hypothesis that Da fused to the C-terminus abolishes the association of Acc1 with the ER membrane. It could also indicate that the protein is not folded correctly. The latter could also explain the lower intensity of the fluorescence, since it's likely that the proteins, when incorrectly folded, are degraded more rapidly. It is unlikely that the difference of intensity is the result of a difference in transcription and/or translation, as the same promoter and terminators are used, and the additionally fused protein domain only comprised a small fraction of the total length of the gene. Vice versa, the difference in intensity could also mean that Acc1** without Da is inadequately degraded. This seems improbable, as this is the more native conformation of the protein, and it has also been reported that the aggregation of Acc1 is a normal response to oxygen or glucose limitation (Tehlivets et al. 2007).

To further investigate the effect of Da fused to the C-terminus of Acc1** and to check whether Acc1**-Da is functional or indeed incorrectly folded, the effect on the 3-HP production was examined. This was done by introducing the MCR_{Ca} gene, which converts malonyl-CoA to 3-HP, on a plasmid (pYC1) into strains with the genomic integration of Acc1** with and without Da fused to the C-terminus, but lacking eGFP fused to the N-terminus. As a control, the plasmid containing MCR_{Ca} was also introduced into the parental CEN.PK113-5D strain. Several different colonies of the three strains were tested in small shake flasks containing 20 mL synthetic medium at an initial OD_{600} of 0.02. The yield of biomass shown in figure 6, expressed as the OD_{600} after 72 hours divided by the amount of glucose initially present in the medium in grams, as measured by HPLC. The yield of OD_{600} over glucose, rather than the final OD_{600}, is presented, because the data was obtained in two separate cultivations, using different batches of medium that were found to vary slightly in glucose content. This way, the data was deemed more consistent. Similarly, the yield of 3-HP over glucose after 72 hours is shown in figure 7. See table A1 for final OD_{600} values and 3-HP titers.

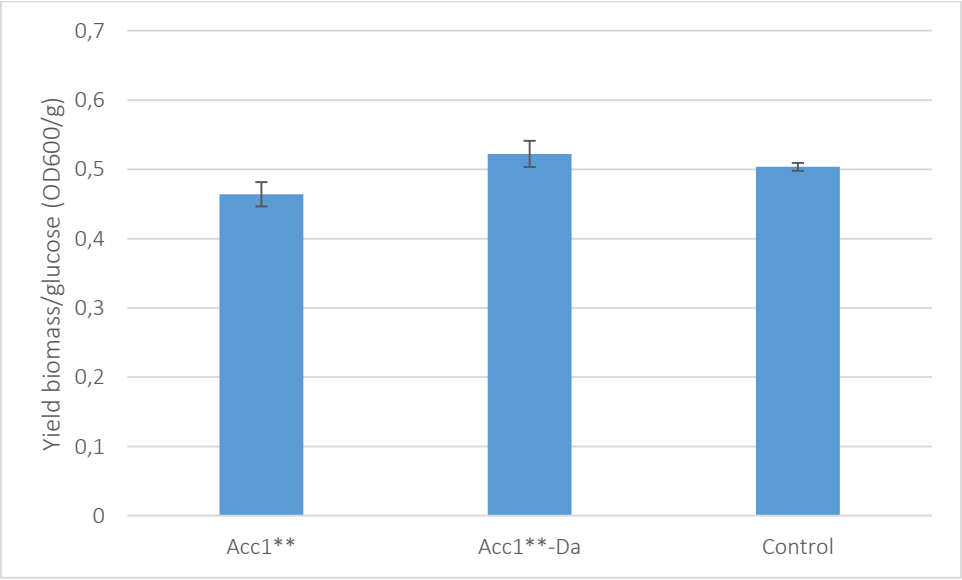

*Figure 6: The biomass yield after 72 hours of cultivation in small shake flasks. The yield is expressed as the OD_{600} divided by the initial amount of glucose in grams. The strains used have Acc1** integrated in the genome, with and without Da fused to the C-terminus of the enzyme, and MCR_{Ca} expressed on a plasmid. The parental CEN.PK113-5D plus MCR_{Ca} was used as a control. The error bars represent the standard deviation. Acc1** = JK0111, Acc1**-Da = JK0211, control = JK0001.*

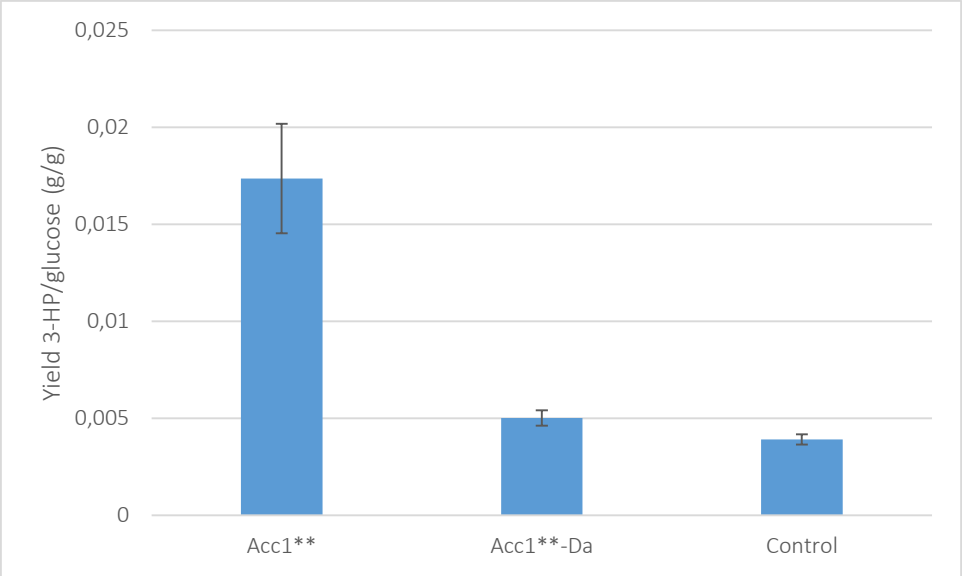

*Figure 7: The 3-HP yield after 72 hours of cultivation in small shake flasks. The yield is expressed as grams of 3-HP divided by the initial amount of glucose in grams. The strains used have Acc1** integrated in the genome, with and without Da fused to the C-terminus of the enzyme, and MCR_{Ca} expressed on a plasmid. The parental CEN.PK113-5D plus MCR_{Ca} was used as a control. The error bars represent the standard deviation. Acc1** = JK0111, Acc1**-Da = JK0211, control = JK0001.*

As can be seen in figure 7, the strain with Acc1** integrated in the genome indeed has an increased production of 3-HP compared to the control strain, which agrees with previously conducted research (Shi et al. 2014). However, the strain that has an integrated copy of Acc1** fused to Da shows no comparable increase in 3-HP production. This leads to the simple conclusion that Acc1** with Da fused to the C-terminus is not functional, which was already implied by the results from the fluoresce microscopy. Whether the non-functionality is the result of incorrect folding or from an interference of the enzymes activity by, for example, blocking the active site cannot be deduced from the cultivation experiment. Yet, the fluorescence microscopy strongly points to the former: incorrect folding.

To test whether Acc1**-Da was not functional because that's an inherent result of fusing any protein to the C-terminus of Acc1** or rather the specific result of the Da dockerin, several new strains were constructed.

eGFP was fused to the C-terminus of Acc1**, in the same manner as was done to create the Yeast GFP Fusion Localization Database (Huh et al. 2003), as this reportedly resulted in a functional enzyme (see figure A2 for their picture), whereas Tehlivets et al. 2007 weren't able to functional express Acc1 with GFP fused to the C-terminus. Additionally, Da was also fused to the N-terminus. Figure 8 shows the result of the fluorescence microscopy with these strains.

	Acc1**-eGFP JK0500	Da-Acc1**-eGFP JK0600
50 ms	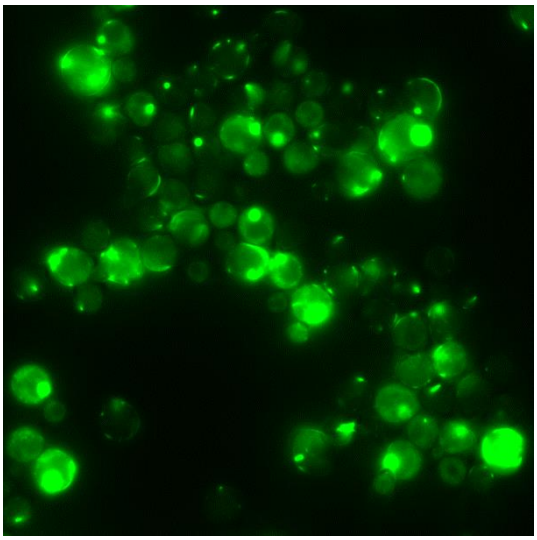	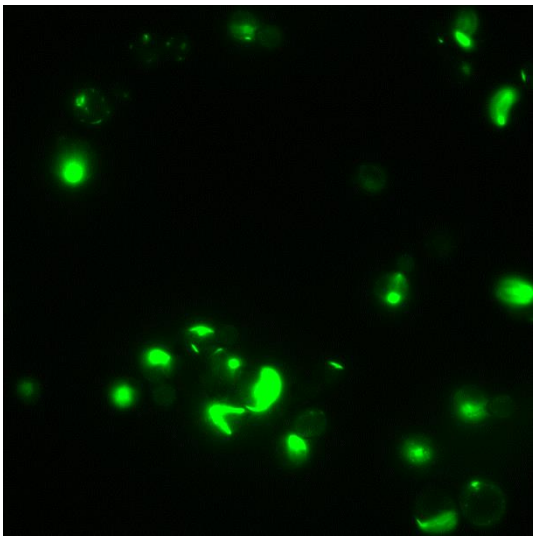
DIC	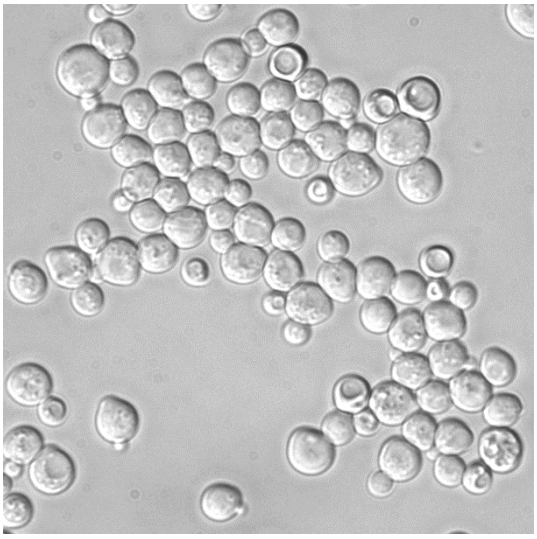	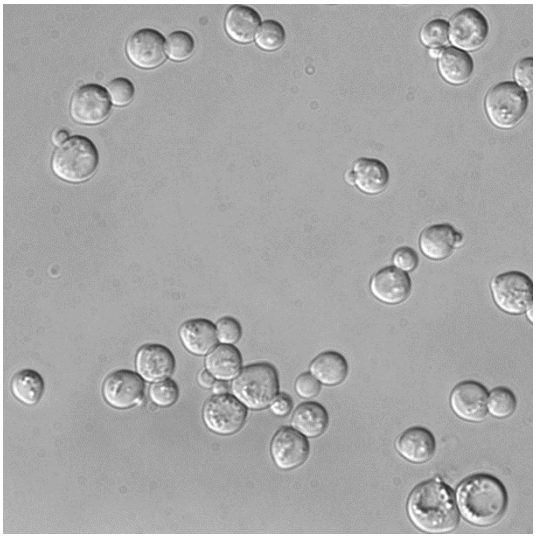

*Figure 8: Result of the fluorescence microscopy of Acc1** with eGFP fused to the C-terminus and with and without Da fused to the N-terminus (JK0600 and JK0500). The bottom image were taken using differential interference contrast (DIC) microscopy.*

As can be seen in figure 8, the distribution of the fluorescence within the cell expressing Acc1**-eGFP resembles the pattern of eGFP-Acc1**, shown in figure 5. Bright spots are formed as well as fibrous structures. Da-Acc1**-eGFP also seems to resemble eGFP-Acc1** and Acc1**-eGFP more closely than eFGP-Acc1**-Da. As Acc1**-Da was not functional, this might suggest that Acc1**-eGFP and even Da-Acc1**-eGFP may well be functional. In order to test this, the Acc1**-eGFP and eGFP-Acc1** strains have been transformed with the plasmid containing the MCR_{Ca} gene to assess the 3-HP production. The results are shown further down in figure 11.

Two strains were constructed expressing the Da dockerin directly fused to eGFP. The first one used the exact same configuration of the dockerin as it was used for the Acc1**-Da strain (eGFP-Da) and the second one lacked the first fourteen amino acids of Da that composed a linker (eGFP-Da^{-14}).Those two strains were also examined using fluorescence microscopy, but interestingly, both strains had a very week fluorescence signal. In order to make sure the constructs were correctly assembled, they were verified by sequencing, proving that they were indeed correctly assembled. This strongly indicates that the Da dockerin, as it has been used in this study, interferes with the protein folding.

In order to get more quantitative results of the fluorescence, all the fluorescent strains were also investigated using flow cytometry. The results are presented in figure 9.

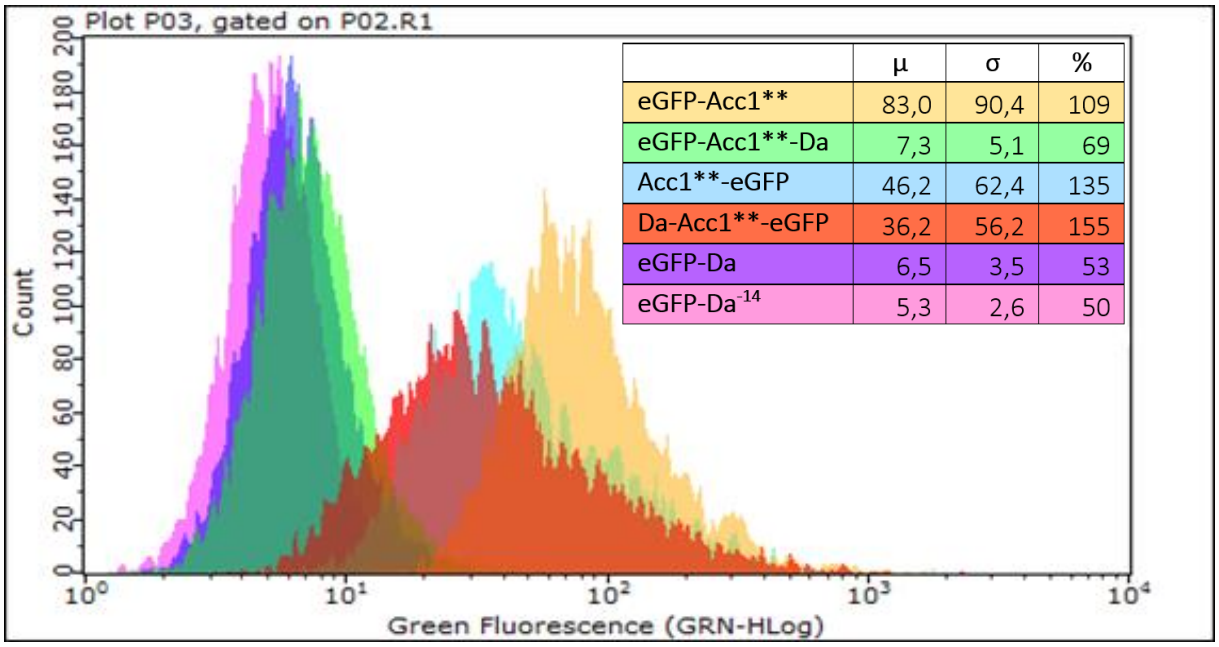

	μ	σ	%
eGFP-Acc1**	83,0	90,4	109
eGFP-Acc1**-Da	7,3	5,1	69
Acc1**-eGFP	46,2	62,4	135
Da-Acc1**-eGFP	36,2	56,2	155
eGFP-Da	6,5	3,5	53
eGFP-Da^{-14}	5,3	2,6	50

*Figure 9: Results of the flow cytometry with the different eGFP-fusion constructs. The table presents the mean value of the fluorescence, the standard deviation and the relative standard deviation (σ/μ) in percentage. eGFP-Acc1** = JK0300, eGFP-Acc1**-Da = JK0400, Acc1**-eGFP = JK0500, Da-Acc1**-eGFP = JK0600, eGFP-Da = JK0900, eGFP-Da^{-14} = JK1000.*

The flow cytometry results clearly support the findings from the microscopy. The strain that has Da fused to the C-terminus of Acc1** has a more than tenfold lower average fluorescence than the strain without, and is comparable to the signal of the strains that have Da directly fused to eGFP. Yet, the stain that has Da fused to the N-terminus has a similar signal compared to the one without.

The large difference in fluorescence between cells of the same strain (i.e. high standard deviation) that was seen in the microscopy pictures is also displayed in results of the flow cytometry. Especially the two strains that have eGFP to the C-terminus have a huge standard deviation. Their mean value is also roughly two-fold lower compared to the strain that has eGFP to the N-terminus.

Finally, to test whether the different Acc1** configurations were actually functional, several of those strains (eGFP-Acc1**, Acc1**-eGFP, Acc1**-Da^{-14}, Da-Acc1**) were also transformed with the plasmid harboring MCR_{Ca} and investigated for 3-HP production, in the same manner as was done with the Acc1** and Acc1**-Da strains (figure 7). The results of these cultivations are shown in figures 10 and 11, where the OD_{600} and the 3-HP concentration after 72 hours divided by the initial glucose concentration are presented.

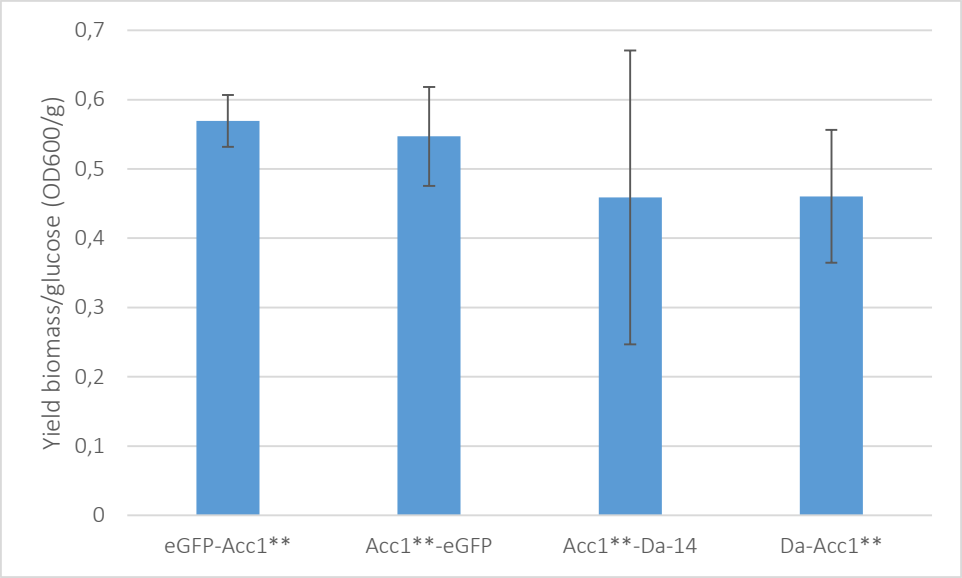

*Figure 10: The biomass yield after 72 hours of cultivation in small shake flasks. The yield is expressed as the OD_{600} divided by the initial amount of glucose in grams. The strains used have Acc1** integrated in the genome in several different configurations, and MCR_{Ca} expressed on a plasmid. The error bars represent the standard deviation. eGFP-Acc1** = JK0311, Acc1**-eGFP = JK0511, Acc1**-Da-14 = JK0811, Da-Acc1** = JK0711.*

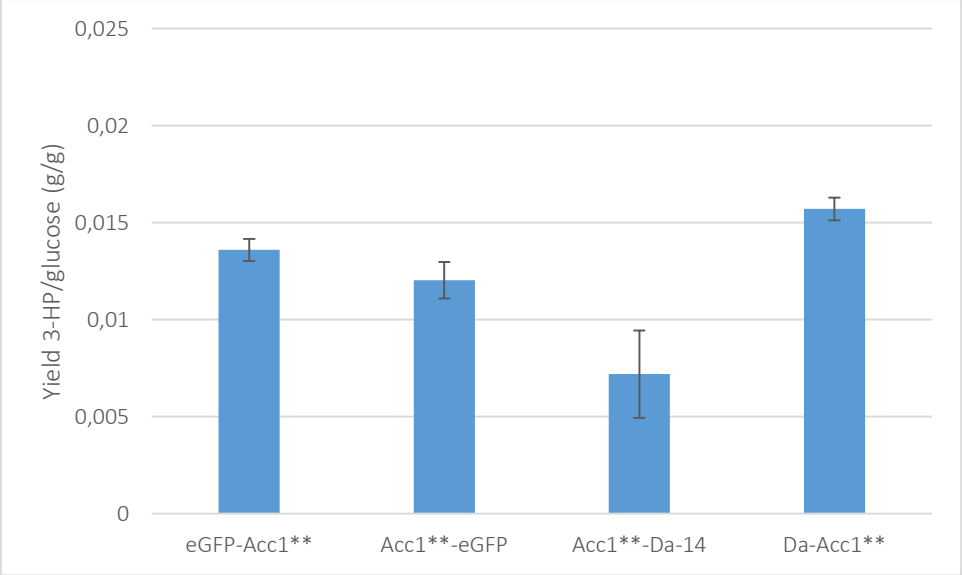

*Figure 11: The 3-HP yield after 72 hours of cultivation in small shake flasks. The yield is expressed as grams of 3-HP divided by the initial amount of glucose in grams. The strains used have Acc1** integrated in the genome in several different configurations, and MCR_{Ca} expressed on a plasmid. The error bars represent the standard deviation. eGFP-Acc1** = JK0311, Acc1**-eGFP = JK0511, Acc1**-Da-14 = JK0811, Da-Acc1** = JK0711.*

The 3-HP yields in figure 8 don't show the same large differences as was seen earlier in figure 7. Yet, it is still clear that the 3-HP yield in the strain with Acc1**-Da^{-14} is significantly lower compared to the others. This suggests that Acc1** is not functional in this configuration, similar to Acc1**-Da (figure 7). Interestingly, as was suggested by the microscopy of Da-Acc1**-eGFP and the flow cytometry (figure 8 and 9), Da-Acc1** does seem to be functional, since the 3-HP yield corresponds to that of Acc1** (figure 7). Both eGFP-Acc1** and Acc1**-eGFP have been reported to be functionally expressed in yeast (Tehlivets et al. 2007; Huh et al. 2003). The results presented here also indicate that both forms are active, as the 3-HP concentration is higher compared to the control strain (figure 6). Although, the

concentration is slightly lower compared to that with Acc1**, suggesting that eGFP fusion slightly lowers the activity of Acc1**.

3.2 Effect of biotinylation on 3-HP production

Acc1 requires biotin to be covalently attached by Bpl1 in order to be active. Limited biotinylation of the overexpressed Acc1** could therefore potentially restrict the full potential of Acc1** activity. To investigate whether the Acc1** is incompletely biotinylated and if its activity can thus be further increased, BPL1 was overexpressed alongside MCR_{Ca} on a plasmid in the strain with integrated Acc1** and cultivations were carried out with different biotin concentrations in the medium. 3-HP production was then used as a measure for the activity of Acc1**. The standard biotin concentration in the synthetic 'Delft' medium is 0.05 mg/l. The apparent K_M of biotin import is 0.079 mg/l, which corresponds to 1.6 fold of the standard biotin concentration (Rogers & Lichstein 1969). The different strains were cultivated with 1, 2, 5, 10 and 100 fold of the standard biotin concentrations, and the results are shown in figure 12. Note that the cultivations with just MCR_{Ca} expressed on a plasmid and with both MCR_{Ca} and BPL1 expressed are obtained from two separate cultivations conducted in identical manner, but with different batches of medium. Hence the normalization for the glucose concentration, which was slightly different for both batches.

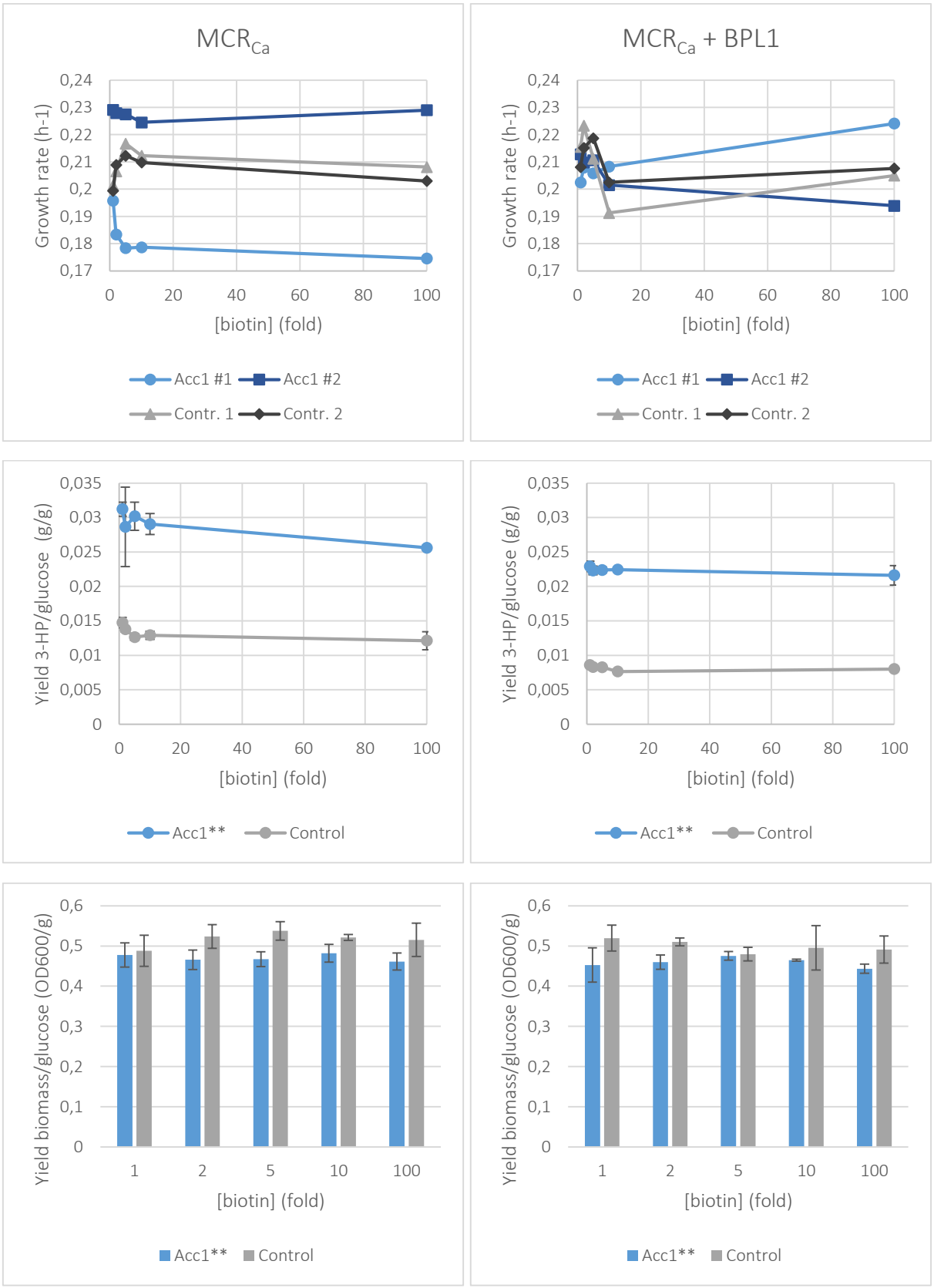

*Figure 12: Growth rate (h^{-1}), 3-HP yield (g/g glucose) and biomass yield (OD_{600}/g glucose) of the strain with Acc1** integrated and expressing MCR_{Ca} and BPL1 on a plasmid, at different concentrations of biotin (fold compared to standard: 0.05 mg/L). Error bars for 3-HP and biomass yields represent the standard deviation of three flasks. The growth rates are from individual flasks, two for the Acc1** strain and two for the control. The results from the left (MCR_{Ca}) and from the right (MCR_{Ca} + BPL1) are obtained from two separate cultivations conducted in identical manner. Strains used: JK0111 (Acc1** + MCR_{Ca}), JK0112 (Acc1** + MCR_{Ca} + BPL1), JK0001 (control + MCR_{Ca}), JK0002 (control + MCR_{Ca} + BPL1).*

It’s clear from the experiments with different biotin concentrations that the increased biotin concentration does not significantly influences the production of 3-HP, as the 3-HP concentration remains constant both with and without overexpression of *BPL1*. The yield of 3-HP on glucose after 72 hours seems to be lower with *BPL1* compared to without *BPL1*, for both the Acc1** strain and the control strain (with just the plasmid). Although the results come from two different cultivations and small differences could thus stem from slight changes in the cultivation conditions, it seems clear that neither the increased biotin concentration, nor the overexpression of *BPL1* seems to have the hypothesized effect of increasing the 3-HP production. The effect of BPL1 seems to be slightly different between the Acc1** strain and the control strain, as the average ratio of the 3-HP yield between Acc1** and the control is 2.7 with BPL1 and 2.2 without.

4 Discussion

4.1 Acc1 localization

It was hypothesized that by using a scaffold to bring Acc1 and MCR_{Ca} together, the 3-HP production could be increased and that the presumed association of Acc1 with the outer side of the ER membrane could be abolished. In order to test this, the aim was to fuse Da to the C-terminus of Acc1 and try to see if this would already abolish the association with the ER. However, from the results presented in this study it seems that the Da domain renders the enzyme nonfunctional, as the increase of 3-HP production when overexpressing Acc1** was not observed in the strain with Da fused to its C-terminus. Consequently, it was not possible to test the effect of a synthetic protein scaffold on the production on 3-HP in this study.

The non-functionality is probably the result of incorrect folding and the subsequent degradation, since the constructs with eGFP fused to the N-terminus had over tenfold lower fluorescence with Da fused to the C-terminus. If Da was only interfering with the enzyme activity by, for example, obstructing the active site, one would expect the fluorescence signal to remain similar. One other possibility could be that Da actively induces its degradation via the proteasome. This seems unlikely, because the construct that had Da fused to the N-terminus (and eGFP to the C-terminus) showed a significantly high fluorescence signal, albeit slightly lower compared to the construct with only eGFP fused to the C-terminus. The Da-Acc1** strain also showed increased production of 3-HP, meaning that Acc1** was functional. The problem, however, with this construct is that it is unknown whether Da is still able to bind to its corresponding cohesin protein, as it is supposed to be fused to the C-terminus of a protein. Since dockerins typically still function with a poly-histidine tag fused to their C-terminus (Tsai et al. 2010), and since it was shown that an N-terminal dockerin fused to the C-terminus of an enzyme was still able to bind to its corresponding cohesin, although with a reduced affinity (Caspi et al. 2009), it could well mean that Da can also work when fused to the N-terminus of Acc1**. It is however not so straight forward to test this. Perhaps it would be better to use an N-terminal dockerin module instead, for example the one derived from *C. thermocellum* xylanase Xyn10Z, which was used in the research mentioned above (Caspi et al. 2009).

Yet, the use of the dockerins and cohesins for the scaffold might not be the best way to go in general, since those proteins are part of extracellular cellulosomes and require Ca^{2+} to bind. Half binding occurs at roughly 500 µM Ca^{2+} (Leibovitz et al. 1997), whereas the cytosolic concentration of Ca^{2+} is kept constant around 50 – 200 nM (Liu 2012). Thus, intracellular Ca^{2+} concentrations are probably too low for binding activity. There are various other protein-protein interaction domain families that could potentially be used for synthetic scaffolds. Whitaker & Dueber (2011) have listed several of them.

It could turn out to be extremely difficult or maybe impossible to use Acc1** in combination with a scaffold, for example as a result of its large size and its different domains, or because it requires to be dimeric/oligomeric to be active, which will be discussed further on. Another strategy in that case could be to steer the overproduction of malonyl-CoA towards 3-HP by secluding the required enzymes in a cellular compartment, for example the mitochondria, which already express Acc2, an Acc1 homolog. Perhaps, with the advance of synthetic biology, it might even be possible in the future to create completely synthetic membrane-bound organelles dedicated to a specific pathway (Siddiqui et al. 2012). The main issue with the use of the mitochondria for the production of 3-HP and other organic acids, however, is the fact that those acids cannot readily diffuse through biological membranes at neutral pH, thus making the export of 3-HP out of the cell even more difficult.

As briefly mentioned before, Acc1 requires to be dimeric/oligomeric in order to be catalytically active, with the dimeric interface laying in the BC domain (Shen et al. 2004). It has even been shown that mammalian ACCase can form large linear polymers with a molecular weight of around 8 million Dalton, consisting of 10-20 of the ACCase dimers (Kwon et al. 2012). Due to the strong homology between human and yeast ACCase (Shen et al. 2004), this tendency of ACCase to form more complex polymers is likely also present in yeast Acc1 and would also explain the fibrous structures and large aggregates observed in the microscopy. The fact that the different constructs were still active (except the one with Da at the C-terminus) implies that those Acc1** conformations are still able to form aggregates, or at least dimers. However, this might not necessarily be the case when the enzyme is also bound to a (large) scaffold that is simultaneously bound to one or several MCR_{Ca} units. It is therefore wise to take this dimerization into account when designing the scaffolds, and perhaps have two Acc1** units bind to the scaffold with linkers that will enable them to align properly. On the other hand, if the scaffold poses no problem for the formation of dimers or even larger structures, this could perhaps temper the beneficial effect of a scaffold because the overexpressed Acc1** double mutant might still be able to interact with the native Acc1 and function in its "native localization", regardless of the scaffold. Of course, this is mainly speculation and you won't know if something will work or not until you try it, which is nicely illustrated by the (non-)functionality of the different constructs in this study.

Several strains were constructed expressing eGFP fused to Acc1** (and directly to Da). The aim was to look into the localization of the Acc1** protein and show a potential change in localization, using fluorescent microscopy. The microscope used didn't have a spatial pinhole, which is used in confocal microscopy to eliminate the out of focus light. Thus, the eGFP outside the focal plane is also excited and detected, causing a lot of background fluorescence and making it harder to look at structures inside the cell. Nevertheless, the photos still show an inhomogeneous distribution of the fluorescence. But the use of confocal microscopy can certainly further increase the amount of details and is definitely worth to consider for future experiments.

It was mentioned that Acc1** localization/aggregation is dependent on the aeration and glucose concentration (Tehlivets et al. 2007), which could affect the results of the microscopy. The high cell density used for the microscopy and the sample preparation (i.e. the use of a glass cover slip) will almost certainly cause or increase oxygen and glucose limitation. Whether this is a problem is of course debatable, but since the construct we were mostly interested in (eGFP-Acc1**-Da) wasn't functional and had a very low fluorescent signal, it is not very relevant here.

The flow cytometry was mainly used to produce more quantitative results from the fluorescent strains, and to confirm the observation from the microscopy. It confirmed the big difference in fluorescence observed between eGFP-Acc1** and eGFP-Acc1**-Da and it also quantified the huge variation in fluorescence within the functional Acc1** strains with eGFP fused to it. Ideally, the results from the flow cytometry should also include a control with just eGFP integrated, to compare the variation, but microscopy with a strain that had GFP integrated in the genome after a galactose inducible promoter already showed much less variation see figure A2. The OD_{600} of the cells was around 4 for all strains when they were taken for analysis in the flow cytometer, meaning that they were in the transition from glucose to ethanol phase, which is not ideal, but since the promoter from PGK1 was used for all the constructs, it's unlikely that this variation results from a difference in expression, as PGK1 promoter expression is very constant at different glucose concentrations (Partow et al. 2010). One explanation for the big variation could be that the degradation of Acc1 is actively regulated by the cell, which could be affected by the growth phase the cells are in (e.g. ethanol or glucose phase). It might therefore be interesting to redo the flow cytometry and take samples at different time points, to be sure the cells are either in the glucose phase or the ethanol phase.

Despite the fact that Acc1**-Da turned out to be non-functional, it was still shown that Acc1** can be functionally expressed with a protein domain fused to either side of the protein. Hence, it is still worth to continue exploring the concept of using a scaffold to channel acetyl-CoA towards 3-HP, which is great, since are plenty of examples where the use of a scaffold led to tremendous increase of product formation (Whitaker & Dueber 2011; Wang & Yu 2012).

4.2 Effect of biotinylation on 3-HP production

The second part of the project was to investigate the effect of the biotinylation of Acc1** on the 3-HP production, since ACCase requires to be biotinylated to be active. Overexpression of Acc1** might mean that the amount of biotin, or the Bpl1 activity in the cell is not sufficient to completely biotinylate Acc1**, hence there might be a possibility to further increase Acc1** activity and subsequent 3-HP production by increasing the biotinylation. This was tested in two ways: by increasing the biotin concentration in the medium (up to 100-fold) and by overexpressing a plasmid harboring *BPL1* in the strain that had Acc1** integrated in the genome and MCR_{Ca} on a plasmid. The final 3-HP concentration was used to assess the activity of Acc1**. No increase of 3-HP production was observed for both tactics. In fact, it seemed that overexpressing BPL1 led to a slight decrease of the 3-HP production. The data from the strains with and without BPL1 are from to two different cultivations, with different batches of medium, and small differences in the results might therefore also be the result from small variations in the conditions. The presented data is normalized for the glucose concentration in the medium, but perhaps small differences in pH could have affected the export of 3-HP. If transport is facilitated, the highest potential ratio of intracellular and extracellular of 3-HP is strongly dependent on the pH in the medium, but this dependency decreases with a lower pH (Maris et al. 2004). Since the pH in the medium decreases during cultivation in shake flasks (i.e. because no base titrant is added), the effect of slight changed in the initial pH of the medium is probably nihil on the final 3-HP concentration.

In the used experimental set-up, both the biotin concentration and the overexpression of BPL1 didn't lead to an increase of the 3-HP production, which was assumed to be related to the Acc1** activity, suggesting that Acc1** activity is not significantly regulated by its biotinylation. However, the lack of an effect on 3-HP production doesn't necessarily mean that the intracellular ACCase activity is not changed. The reason for this is that the 3-HP production is the result of a pathway compromised of several reaction, and the overall rate is (mostly) determined by the slowest reaction, rather than a combination or average of the rates of the several steps. So, if the step from malonyl-CoA to 3-HP by MCR_{Ca} is limiting, increased malonyl-CoA production by Acc1** won't increase the 3-HP production because all MCR_{Ca} are already saturated. If the formation of acetyl-CoA or NADPH is limiting, increasing the activity of Acc1** won't increase 3-HP production because the limited amount of acetyl-CoA/NADH remain the same, regardless of Acc1** activity. The first case seems unlikely, since MCR_{Ca} is expressed on a plasmid, whereas Acc1** has only a single copy integrated in the genome. However, the latter case is not that unlikely. It has already been shown that increasing the NADPH supply, by overexpressing a non-phosphorylating glyceradehyde-3-phosphate dehydrogenase (GAPN), increases the 3-HP production by 70% in a strain that had several genes in the pathway to malonyl-CoA overexpressed, which is comparable to the effect of Acc1** (Chen et al. 2014). Therefore, to be conclusive about the effect of the increased biotin concentration and the overexpression of *BPL1*, the activity of ACCase should be measured directly by doing an enzyme activity assay.

The growth rate and the final biomass concentration also seemed to be unaffected by the overexpression of *BPL1* on a plasmid. This was a rather unexpected result, as the simultaneous overexpression of Acc1** and BPL1 was said the render the cells inviable (Tehlivets et al. 2007). Even if the additional expression of MCR_{Ca} could somehow save the cells by perhaps consuming the excessive amount of malonyl-CoA, one would still expect to see an effect on the growth and biomass yield. I

therefore suspect that either something might be wrong with expression of the BPL1 gene on the plasmid, or the statement that simultaneous overexpression of Acc1** and BPL1 renders the cells inviable might be incorrect. It is therefore be wise to double check the plasmid that was used in this study.

4.3 Conclusion

The aim of the study was summarized in three research questions:

1) Is it possible to abolish the association of Acc1 with the ER membrane by fusing Acc1 to a docking domain?
2) Is the 3-HP production improved when Acc1 is linked to MCR_{Ca} via a protein scaffold?
3) To what extend is Acc1** activity regulated by the efficiency of its biotinylation by Bpl1?

Due to the limited time of the project it was not possible to adequately address the proposed questions. However, it was clear that it was not possible to effectively abolish the presumed association of Acc1** with the ER membrane by fusing dockerin a from *C. thermocellum* endoglucanase to the C-terminus of Acc1**, as it rendered to enzyme non-functional, most likely as the result of incorrect folding. The non-functionality of Acc1**-Da was not an inherent feature of Acc1** when fusing a protein domain to the C-terminus, as Acc1** was still functional with eGFP fused to the C-terminus, making the use of a scaffold still a viable strategy to improve the production of 3-HP and other malonyl-CoA derived products.

Cultivating *S. cerevisiae* with Acc1** integrated in the genome in the presence of different biotin concentrations did not lead to an increased production of 3-HP, both with and without overexpressing *BPL1* on a plasmid. This suggested that Acc1** activity is not significantly regulated by its biotinylation. However, to be conclusive about the ACCase activity, it should be directly measured, rather than indirectly, as the 3-HP production is affected by more than just the activity of Acc1**.

4.4 Recommendations for future work

The work that was carried out for this study left some initial questions unanswered and also conceived plenty of new ones. Based on that, and on the literature that I studied I have some recommendations regarding the continuation of this project.

Firstly, I recommend using a different protein-protein interaction to form the basis of the scaffold. Mainly based on the possible low affinity of the dockerin and cohesin interaction as a result of the intracellular Ca^{2+} concentration, which is likely too low. Even if it's not too low, it's probably still safer to use protein (domains) that have been proven to work intracellularly in *S. cerevisiae*, such as SH3 (Wang & Yu 2012).

For the design of the synthetic protein scaffolds it's probably wise to consider the complex nature of Acc1** and its supramolecular structures, as it requires to be dimeric to be catalytically active, while at the same time it's desired to divert the enzyme from its native function within the fatty acid synthesis.

To investigate the localization using GFP and fluorescent microscopy, the use of a confocal microscope will significantly improve the level of detail that can be realized.

It might be good to redo the flow cytometry, and analyze the cells when they have a lower OD_{600} in order to make sure the cells are still in the glucose phase, rather than the transition between glucose and ethanol phase.

In order to be conclusive about the effect of the increased biotin concentrations and the overexpression of *BPL1* on the activity of Acc1**, the ACCase activity should be determined directly in an enzyme activity assay as performed by Shi et al. 2014. Since the enzyme activity is probably rather tricky to do, it might also be worthwhile to first try to see if the expression of GAPN could alleviate a potential NADPH limitation, which would link the 3-HP production again to the activity of Acc1**.

Finally, it is wise to double check the pJK1 plasmid, containing MCR_{Ca} and *BPL1*, via sequencing, to make sure *BPL1* is properly expressed.

5 Acknowledgements

For the past six months I have been conducting the work of my master's thesis at the division of Systems and Synthetic Biology as a visiting researcher. I would like to thank everybody for the great time I have had here, and for answering all my questions along the way. In particular I would like to thank Yun Chen for being my direct supervisor and for all his efforts he took in guiding me. Of course, I would also like to thank Jens Nielsen for accepting me in his research group. It was a great experience, from which I have learned a great deal. Finally, I would also like to thank Oliver Englund Örn for helping me find my way in the beginning, and for sharing his material with me.

6 References

Abu-Elheiga, L. et al., 2001. Continuous fatty acid oxidation and reduced fat storage in mice lacking acetyl-CoA carboxylase 2. *Science (New York, N.Y.)*, 291(5513), pp.2613–2616.

Caspi, J. et al., 2009. Effect of linker length and dockerin position on conversion of a Thermobifida fusca endoglucanase to the cellulosomal mode. *Applied and Environmental Microbiology*, 75(23), pp.7335–7342.

Chen, Y. et al., 2014. Coupled incremental precursor and co-factor supply improves 3-hydroxypropionic acid production in Saccharomyces cerevisiae. *Metabolic Engineering*, 22, pp.104–109. Available at: http://dx.doi.org/10.1016/j.ymben.2014.01.005.

Clark, S., 2014. Global Acrylic Acid Market (Derivatives Types, End Users and Geography) - Size, Share, Global Trends, Company Profiles, Demand, Insights, Analysis, Research, Report, Opportunities, Segmentation and Forecast, 2013 - 2020. *Allied Market Research*. Available at: http://www.alliedmarketresearch.com/acrylic-acid-market [Accessed July 31, 2015].

Fonzi, W.A. & Irwin, M.Y., 1993. Isogenic Strain Construction and Gene Mapping in Candida albicans. *Proceedings of the Royal Society of Medicine*, 134(3), pp.717, 728.

Gietz, R.D. & Schiestl, R.H., 2007. High-efficiency yeast transformation using the LiAc/SS carrier DNA/PEG method. *Nat. Protocols*, 2(1), pp.31–34. Available at: http://dx.doi.org/10.1038/nprot.2007.13.

Hardie, D.G., 2007. AMP-activated/SNF1 protein kinases: conserved guardians of cellular energy. *Nature reviews. Molecular cell biology*, 8(10), pp.774–785.

Hofbauer, H.F. et al., 2014. Regulation of gene expression through a transcriptional repressor that senses acyl-chain length in membrane phospholipids. *Developmental Cell*, 29, pp.729–739.

Hoja, U. et al., 2004. HFA1 encoding an organelle-specific acetyl-CoA carboxylase controls mitochondrial fatty acid synthesis in Saccharomyces cerevisiae. *Journal of Biological Chemistry*, 279(21), pp.21779–21786.

Huh, W.-K. et al., 2003. Global analysis of protein localization in budding yeast. *Nature*, 425, pp.686–691.

Ivessa, A.S., Schneiter, R. & Kohlwein, S.D., 1997. Yeast acetyl-CoA carboxylase is associated with the cytoplasmic surface of the endoplasmic reticulum. *European journal of cell biology*, 74(4), p.399—406. Available at: http://europepmc.org/abstract/MED/9438137.

Jensen, N. et al., 2014. Microbial production of 3-hydroxypropionic acid.

Jiang, X., Meng, X. & Xian, M., 2009. Biosynthetic pathways for 3-hydroxypropionic acid production. *Applied Microbiology and Biotechnology*, 82(6), pp.995–1003.

Kozak, B.U. et al., 2014. Engineering Acetyl Coenzyme A Supply : Functional Expression of a Bacterial Pyruvate Dehydrogenase Complex in the Cytosol of Saccharomyces cerevisiae. , 5(5), pp.1–11.

Krivoruchko, A. & Nielsen, J., 2015. Production of natural products through metabolic engineering of Saccharomyces cerevisiae. *Current Opinion in Biotechnology*, 35, pp.7–15. Available at: http://linkinghub.elsevier.com/retrieve/pii/S0958166914002195.

Kumar, V., Ashok, S. & Park, S., 2013. Recent advances in biological production of 3-hydroxypropionic acid. *Biotechnology Advances*, 31(6), pp.945–961. Available at: http://dx.doi.org/10.1016/j.biotechadv.2013.02.008.

Kwon, S.J., Cho, Y.S. & Heo, Y.-S., 2012. Structural Insights into the Regulation of ACC2 by Citrate. *Bulletin of the Korean Chemical Society*, 34(2), p.565.

Langeveld, J.W. a., Dixon, J. & Jaworski, J.F., 2010. Development Perspectives Of The Biobased Economy: A Review. *Crop Science*, 50(Supplement 1), p.S–142–S–151.

Leibovitz, E. et al., 1997. Characterization and subcellular localization of the Clostridium thermocellum scaffoldin dockerin binding protein sdbA. *Journal of Bacteriology*, 179(8), pp.2519–2523.

Liu, W., 2012. Control of Calcium in Yeast Cells. In *Introduction to Modeling Biological Cellular Control Systems SE - 5*. MS&A. Springer Milan, pp. 95–122. Available at: http://dx.doi.org/10.1007/978-88-470-2490-8_5.

Maris, A.J. a Van et al., 2004. Microbial export of lactic and 3-hydroxypropanoic acid: Implications for industrial fermentation processes. *Metabolic Engineering*, 6, pp.245–255.

Mikkelsen, M.D. et al., 2012. Microbial production of indolylglucosinolate through engineering of a multi-gene pathway in a versatile yeast expression platform. *Metabolic Engineering*, 14(2), pp.104–111. Available at: http://dx.doi.org/10.1016/j.ymben.2012.01.006.

Partow, S. et al., 2010. Characterization of different promoters for designing a new expression vector in Saccharomyces cerevisiae. *Yeast*, 27, pp.955–964.

Podkowiński, J. & Tworak, A., 2011. Acetyl-coenzyme A carboxylase - an attractive enzyme for biotechnology. *Biotechnologia*, 92(4), pp.321–335.

Rogers, T.O. & Lichstein, H.C., 1969. Characterization of the biotin transport system in Saccharomyces cerevisiae. *Journal of Bacteriology*, 100(2), pp.557–564.

Shen, Y. et al., 2004. A mechanism for the potent inhibition of eukaryotic acetyl-coenzyme A carboxylase by soraphen A, a macrocyclic polyketide natural product. *Molecular Cell*, 16(6), pp.881–891.

Shi, S. et al., 2014. Improving production of malonyl coenzyme A-derived metabolites by abolishing Snf1-dependent regulation of Acc1. *mBio*, 5(3), pp.1–8.

Siddiqui, M.S. et al., 2012. Advancing secondary metabolite biosynthesis in yeast with synthetic biology tools. *FEMS Yeast Research*, 12(2), pp.144–170.

Tehlivets, O., Scheuringer, K. & Kohlwein, S.D., 2007. Fatty acid synthesis and elongation in yeast. *Biochimica et Biophysica Acta - Molecular and Cell Biology of Lipids*, 1771, pp.255–270.

Tong, L., 2005. Acetyl-coenzyme A carboxylase: Crucial metabolic enzyme and attractive target for drug discovery. *Cellular and Molecular Life Sciences*, 62(16), pp.1784–1803.

Tsai, S.L., Goyal, G. & Chen, W., 2010. Surface display of a functional minicellulosome by intracellular complementation using a synthetic yeast consortium and its application to cellulose hydrolysis and ethanol production. *Applied and Environmental Microbiology*, 76(22), pp.7514–7520.

Wang, Y. & Yu, O., 2012. Synthetic scaffolds increased resveratrol biosynthesis in engineered yeast cells. *Journal of Biotechnology*, 157(1), pp.258–260. Available at: http://dx.doi.org/10.1016/j.jbiotec.2011.11.003.

Verduyn, C. et al., 1992. Effect of Benzoic Acid on Metabolic Fluxes in Yeasts: A Continuous-Culture Study on the Regulation of Respiration and Alcoholic Fermentation. *Yeast*, 8(7), pp.501–517.

Werpy, T. & Petersen, G., 2004. Top Value Added Chemicals from Biomass Volume I — Results of Screening for Potential Candidates from Sugars and Synthesis Gas Top Value Added Chemicals From Biomass Volume I : Results of Screening for Potential Candidates. , 1.

Whitaker, W.R. & Dueber, J.E., 2011. *Metabolic pathway flux enhancement by synthetic protein scaffolding* 1st ed., Elsevier Inc. Available at: http://dx.doi.org/10.1016/B978-0-12-385075-1.00019-6.

Zhang, J., Vemuri, G. & Nielsen, J., 2010. Systems biology of energy homeostasis in yeast. *Current Opinion in Microbiology*, 13(3), pp.382–388. Available at: http://dx.doi.org/10.1016/j.mib.2010.04.004.

7 Appendix

*Table A1: Results of the cultivation with the different conformations of Acc1**, to test if they are functional, by expressing MCR_{Ca} on a plasmid and measuring the 3-HP production. OD_{600} and 3-HP concentration after 72 hours cultivation in shake flasks plus the glucose concentration in the medium as measured by HPLC.*

Strain	Average final OD	Standard deviation	Average final [3-HP]	Standard deviation	[Glucose] in medium
	OD_{600}	OD_{600}	g/l	g/l	g/l
Acc1**	8.02	0.30	0.300	0.049	17.3
Acc1**-Da	10.54	0.38	0.101	0.008	20.2
Control	10.16	0.12	0.079	0.005	20.2
eGFP-Acc1**	10.88	0.71	0.260	0.011	19.1
Acc1**-eGFP	10.45	1.37	0.230	0.018	19.1
Acc1**-Da-14	8.77	4.05	0.137	0.043	19.1
Da-Acc1**	8.80	1.83	0.300	0.011	19.1

Table A2: Results of the cultivation at different biotin concentrations. OD_{600} and 3-HP concentration after 72 hours cultivation in shake flasks plus the glucose concentration in the medium as measured by HPLC. Values are presented with the standard deviation.

Biotin			1x	2x	5x	10x	100x	[Glucose] (g/l)
OD_{600}	MCR	Acc1**	8.59 ± 0.54	8.37 ± 0.43	8.40 ± 0.33	8.67 ± 0.39	8.29 ± 0.38	16.0
		Control	8.77 ± 0.70	9.41 ± 0.53	9.67 ± 0.41	9.37 ± 0.13	9.27 ± 0.75	16.0
	MCR +BPL	Acc1**	8.47 ± 0.80	8.60 ± 0.33	8.89 ± 0.20	8.69 ± 0.05	8.29 ± 0.21	18.7
		Control	9.72 ± 0.60	9.55 ± 0.19	8.97 ± 0.31	9.27 ± 1.04	9.19 ± 0.63	18.7
[3HP] (g/l)	MCR	Acc1**	0.499 ± 0.016	0.458 ± 0.092	0.483 ± 0.033	0.464 ± 0.024	0.409 ± 0.006	16.0
		Control	0.236 ± 0.012	0.220 ± 0.006	0.202 ± 0.008	0.206 ± 0.009	0.194 ± 0.021	16.0
	MCR +BPL	Acc1**	0.429 ± 0.014	0.418 ± 0.012	0.419 ± 0.008	0.420 ± 0.004	0.405 ± 0.026	18.7
		Control	0.161 ± 0.005	0.155 ± 0.006	0.155 ± 0.006	0.143 ± 0.005	0.150 ± 0.006	18.7

*Table A3: List of primers used for the construction of the integration cassettes. * 1 = Acc1**, 2 = Acc1**-Da, 3 = eGFP-Acc1**, 4 = eGFP-Acc1**-Da, 5 = Acc1*-Da, 6 = Da-Acc1**-eGFP, 7 = Da-Acc1**, 8 = Acc1**-Da^{-14}, 9 = eGFP-Da, 10 = eGFP-Da^{-14}*

#nr	Oligo name	Overhang	Used for*	Sequence
1	1)pPGK1, fwd	X2-up	1, 2, 3, 4, 5, 6, 7, 8, 9, 10	AGAGAAACTCGCAGGCAACTTGCTCTCGAAGTGGTCACGTGGAAGTACCTTCAAAGAATGGGGTC
2	2)pPGK1, rev	eGFP	3, 4, 9, 10	GTTCTTCTCCTTTACTGTTAATTAACCCGGGGATTCGCATTTGTTTTATATTTGTTGTAAAAAGTAGATAATTACTTCCTTG
3	3)Acc1**, rev		1, 2, 3, 4, 5, 6, 7, 8	TTTCAAAGTCTTCAACAATTTTTCTTTATCATCG
4	4)eGFP, rev	eGFP	3, 4, 9, 10	TGAACCAGAACCGCTGCCGGATCCTTTGTATAGTTCATCCATGCCATGTG
5	5)Acc1**, fwd	eGFP+linker	3, 4	GGATGAACTATACAAAGGATCCGGCAGCGGTTCTGGTTCAATGAGCGAAGAAAGCTTATTCGA
6	6)X2-up, fwd		1, 2, 3, 4, 5, 6, 7, 8, 9, 10	CGTCTATGAGGAGACTGTTAGTTGG
7	7)X2-up, rev		1, 2, 3, 4, 5, 6, 7, 8, 9, 10	ACGTGACCACTTCGAGAGCA
8	8)X2-down, fwd		2, 4, 5, 6, 8, 9, 10	ATCCGCTCTAACCGAAAAGGAAG
9	9)X2-down, fwd	Acc1**	1, 3, 7	ATCTACCGATGATAAAGAAAAATTGTTGAAGACTTTGAAATAAATCCGCTCTAACCGAAAAGGAAG
10.2	10.2)X2-down, rev		1, 2, 3, 4, 5, 6, 7, 8, 9, 10	CATTACCATCCCATGTAAGAACGGA
11	11)Da, fwd	Acc1**	2, 4	ATCTACCGATGATAAAGAAAAATTGTTGAAGACTTTGAAATCAGGTCAACCTACTCCACCTTCTAAC
12	12)Da, rev	X2-down (tCYC1)	2, 4, 8, 9, 10	TTCAGGTTGTCTAACTCCTTCCTTTTCGGTTAGAGCGGATTCAGTAAGGTAAGTGAGGGATGGATTTGATTAA
13	13)eGFP, fwd		3, 4, 9	ATGCGAATCCCCGGGTTAATT
15	15)Acc1** mid, rev		1, 2, 3, 4, 5, 6, 7, 8	TGGTTCAGAGCGCTTTGGATTG
16	16)Acc1** mid, fwd		1, 2, 3, 4, 5, 6, 7, 8	TAAGGCTACCGCTAAGGTCGC
45	eGFP fwd, Acc1 homology	Acc1**	5, 6	ATCTACCGATGATAAAGAAAAATTGTTGAAGACTTTGAAACGAATCCCCGGGTTAATTAACAG
46	eGFP rev		9, 10	TTTGTATAGTTCATCCATGCCATGTG
47	eGFP rev, tCYC1 homology	tCYC1	5, 6	CTAACTCCTTCCTTTTCGGTTAGAGCGGATTCATTTGTATAGTTCATCCATGCCATGTG
48	Da fwd, eGFP homology	eGFP	9, 10	ATTACACATGGCATGGATGAACTATACAAATCAGGTCAACCTACTCCACCTTCTAAC
49	Da(min 14 aa) fwd, eGFP homology	eGFP	10	ATTACACATGGCATGGATGAACTATACAAACCACCTCAAGTAGTTTATGGTGACG
50	Da(min 14 aa) fwd, Acc1 homology	Acc1**	8	ATCTACCGATGATAAAGAAAAATTGTTGAAGACTTTGAAACCACCTCAAGTAGTTTATGGTGACG
51	pPGK1 rev		6, 7	TTGTTTTATATTTGTTGTAAAAAGTAGATAATTACTTCCTTG
52	Acc1 fwd. Da-linker homology	Da+linker	6, 7	CCTTACGGATCCGGCAGCGGTTCTGGTTCAATGAGCGAAGAAAGCTTATTCGA
53	Da fwd, pPGK1 homolgy, start c	pPGK1	6, 7	CAAGGAAGTAATTATCTACTTTTTACAACAAATATAAAACAAATGTCAGGTCAACCTACTCCACCTTCTAAC
54	Da rev, linker		6, 7	TGAACCAGAACCGCTGCCGGATCCGTAAGGTAAGTGAGGGATGGATTTG

Table A4: List of primers used for plasmid construction.

#nr	Oligo name	Overhang	Used for	Sequence
55	BPL1 fwd – NotI	NotI	pJK1	ACTGAgcggccgcCAAAATGAATGTATTAGTCTATAATGGCCCAGG
56	BPL1 rev – PacI	PacI	pJK1	GGCCGttaattaaTTAACTCTGAACCTTTTTAGCAATTAAGCTC

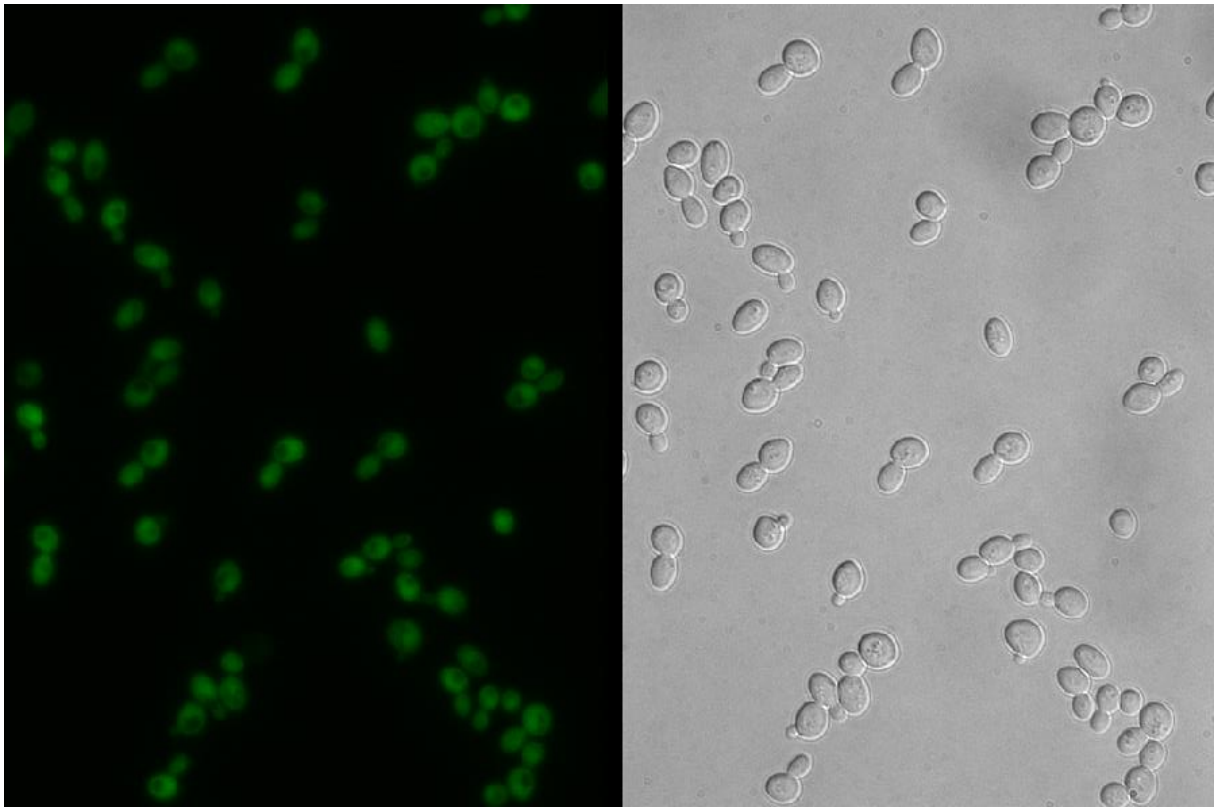

Figure A1: Fluorescence microscopy of cells with an integrated copy of GFP, controlled by a galactose inducible promoter.

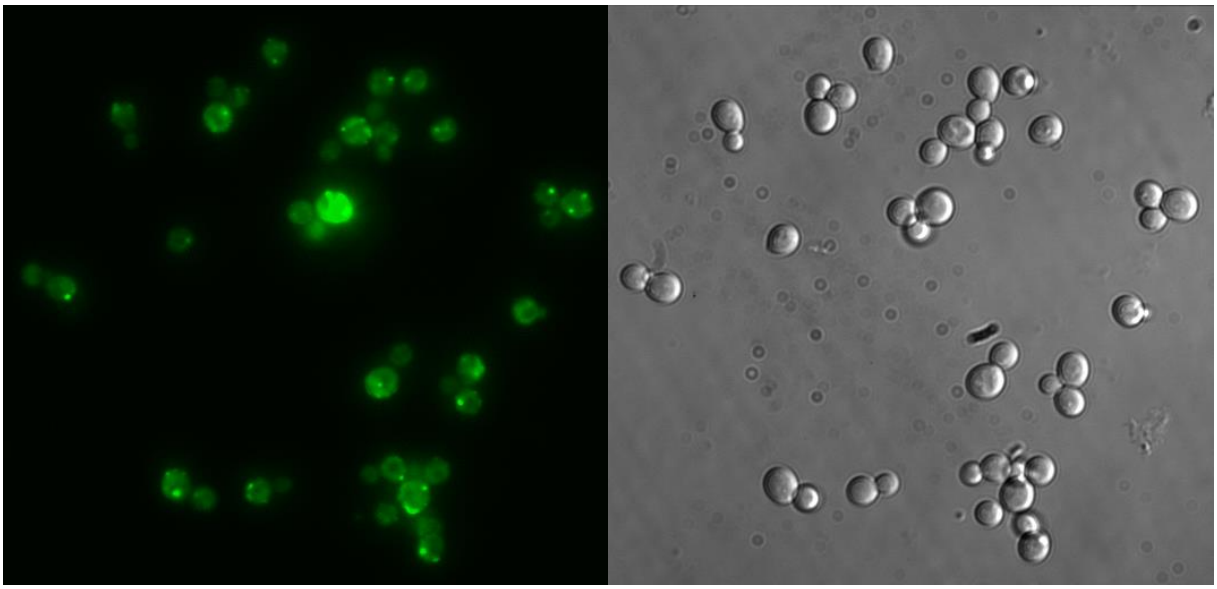

Figure A2: Image of Acc1 fused to GFP from the Yeast GFP Localization Database (Huh et al. 2003)*. Copied at 2015-08-13 from: http://yeastgfp.yeastgenome.org/displayLocImage.php?loc=16531*

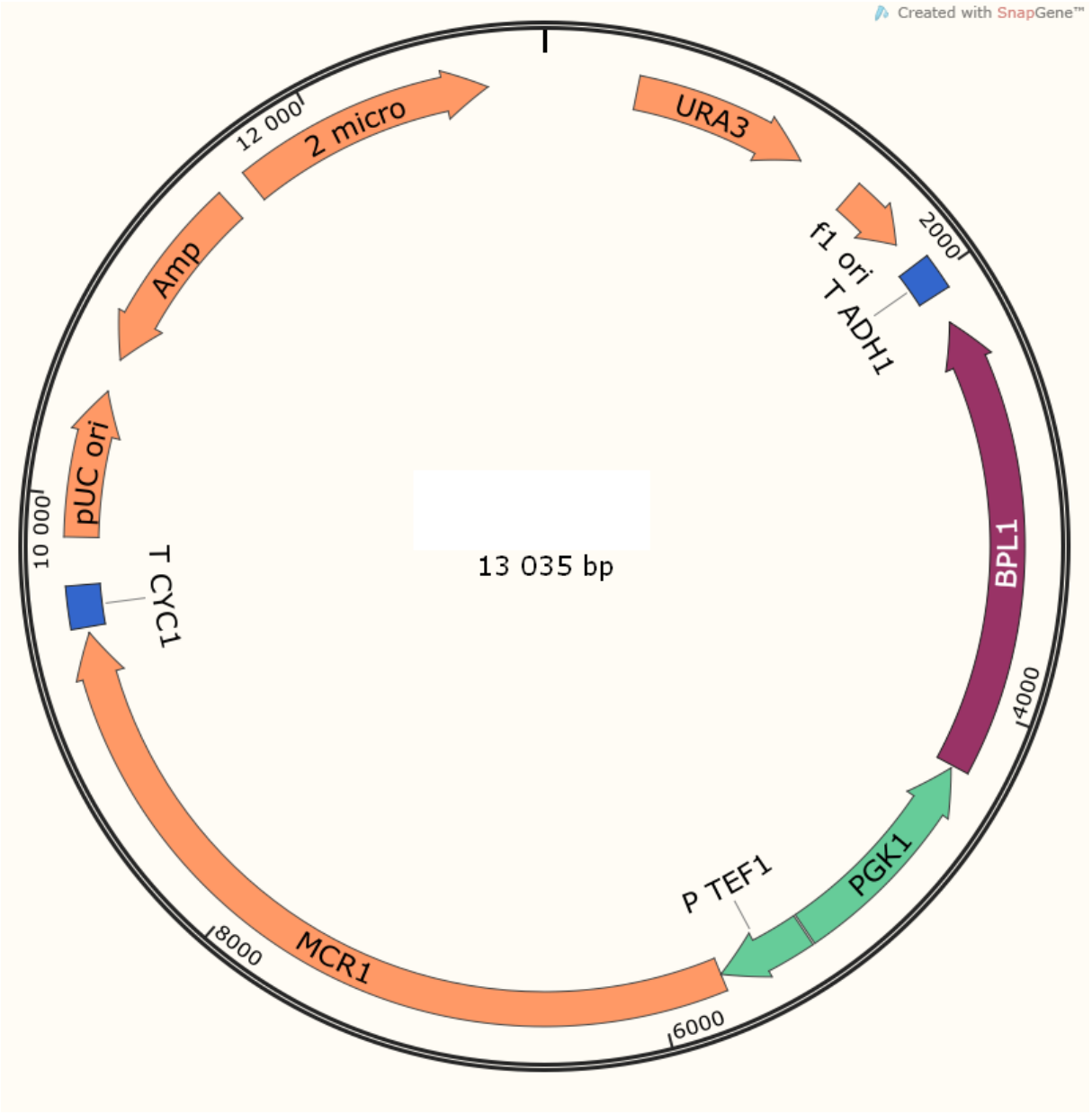

Figure A3: Plasmid map of pJK1.